

Manuscript Number: JAES-D-20-00152R3

Title: Seismostratigraphic architecture of the Sulaiman Fold-Thrust Belt Front (Pakistan): Constraints for resource potential of the Cretaceous-Paleogene strata in the East Gondwana Fragment

Article Type: Research Paper

Keywords: foreland basin; seismic; Pakistan.

Corresponding Author: Dr. Natasha Khan, Ph.D.

Corresponding Author's Institution: University of Peshawar

First Author: Natasha Khan, Ph.D.

Order of Authors: Natasha Khan, Ph.D.; Nicola Scarselli, Ph.D.

Abstract: Interpretation of seismic reflection profiles tied to well controls allowed assessing the stratigraphic and structural style of the Sulaiman Fold-Thrust Belt (SFTB) including the Zindapir Anticline (ZA) and the adjacent Sulaiman Foredeep. Seismic attributes and facies analysis have shown that in the subsurface of the Sulaiman Foredeep, the presence of shallow marine shelfal deposits is seismically characterized by well-imaged prograding systems of the Paleocene-Eocene age. This same stratigraphic unit also contains packages of divergent reflections fanning towards the west, forming a prominent stratigraphic thickness expansion. The presence of prograding units and the occurrence of stratigraphic thickening are explained with a phase of accelerated subsidence, likely related to an early stage of the SFTB orogeny during the Indian Plate-Afghan Block collision that caused crustal flexure and the formation of an initial foreland basin to the east. Progressive deformation towards the east is evidenced by well-developed, 2-14 km wide, Neogene faulted-detachment folds in the ZA area, that contrast with open folds of the same age observed further to the east, affecting the near surface strata. This recent deformation event may indicate the influence of the Indian-Afghan collisional tectonics during the Oligocene-Miocene. The evolution of the SFTB in this study has significant implications for exploration of new petroleum plays.

Research Data Related to this Submission

There are no linked research data sets for this submission. The following reason is given:

The authors do not have permission to share data

1 **Highlights**

- 2 • Tectono-stratigraphic evolution and resource potential of the northwestern margin of the
3 Indian Plate is described.
- 4 • The Sulaiman Fold-Thrust Belt forms a thin-skinned system controlled by two key
5 detachments in the Cretaceous and Eocene strata.
- 6 • Structural style of the fold belt dominated by detachment folds developed within an
7 overall eastward migrating deformation front.
- 8 • In the Sulaiman Foredeep, thickening and occurrence of westward migrating prograding
9 units in the Paleogene succession provide evidence for crustal loading.
- 10 • The **Cenozoic** petroleum exploration plays are varied due to complex tectonic setup from
11 west to east.

12
13
14
15

ACCEPTED MANUSCRIPT

1 **Seismostratigraphic architecture of the Sulaiman Fold-Thrust Belt Front (Pakistan):**

2 **Constraints for resource potential of the Cretaceous-Paleogene strata in the East**

3 **Gondwana Fragment**

4
5 Natasha Khan^a, Nicola Scarselli^b

6 a. National Centre of Excellence in Geology, University of Peshawar, Peshawar, 25130,
7 Pakistan

8 b. Fault Dynamics Research Group, Department of Earth Sciences, Queen's Building,
9 Royal Holloway University of London, Egham, Surrey, TW20 0EX, United Kingdom

10 11 **Abstract**

12 Interpretation of seismic reflection profiles tied to well controls allowed assessing the
13 stratigraphic and structural style of the Sulaiman Fold-Thrust Belt (SFTB) including the Zindapir
14 Anticline (ZA) and the adjacent Sulaiman Foredeep. Seismic attributes and facies analysis have
15 shown that in the subsurface of the Sulaiman Foredeep, the presence of shallow marine shelfal
16 deposits is seismically characterized by well-imaged prograding systems of the Paleocene–
17 Eocene age. This same stratigraphic unit also contains packages of divergent reflections fanning
18 towards the west, forming a prominent stratigraphic thickness expansion. The presence of
19 prograding units and the occurrence of stratigraphic thickening are explained with a phase of
20 accelerated subsidence, likely related to an early stage of the SFTB orogeny during the Indian
21 Plate-Afghan Block collision that caused crustal flexure and the formation of an initial foreland
22 basin to the east.

23 Progressive deformation towards the east is evidenced by well-developed, 2–14 km wide,
24 Neogene faulted-detachment folds in the ZA area, that contrast with open folds of the same age
25 observed further to the east, affecting the near surface strata. This recent deformation event may
26 indicate the influence of the Indian-Afghan collisional tectonics during the Oligocene–Miocene.
27 **The evolution of the SFTB in this study has significant implications for exploration of new**
28 **petroleum plays.**

29 **Key words:** foreland basin, seismic, Pakistan.

30 **1. Introduction**

31 The Sulaiman Basin, recognized as a prolific hydrocarbon basin is a part of the Sulaiman Fold-
32 Thrust Belt System (SFTB) and the adjacent Sulaiman Foredeep with a characteristic festoon-
33 like arcuate architecture termed as the Sulaiman Lobe and the Sulaiman Arc in the literature
34 (Crawford, 1974; Sarwar and DeJong, 1979; Reynolds et al., 2015) (Fig. 1). The stratigraphy of
35 the eastern Sulaiman Basin, which is the focus of this paper, comprises of the Cretaceous and
36 Paleogene mixed clastics and carbonate successions (Fig. 2). The region encompasses the
37 northwestern margin of the Indian Plate (Gondwanian Domain) and is under the influence of the
38 constant tectonic motion of Indian-Eurasian Plates and the Afghan Block. The tectonic setting of
39 the area displays a compressional basin with a strike-slip component (Banks and Warburton,
40 1986; Humayun et al., 1991; Jadoon et al., 1992). Worldwide examples of similar arcuate
41 tectonic domains include the Zagros Foredeep of Iran, the Mesopotamian Foredeep of Iraq, the
42 Omani Foredeep and the Polish Carpathians Foredeep.

43 Previous research on the Sulaiman Fold-Thrust Belt (SFTB), Zindapir Anticline and the adjacent
44 Sulaiman Foredeep is primarily driven by petroleum exploration and mainly focuses on the

45 structural geometry, satellite and outcrop based stratigraphy (Banks and Warburton, 1986;
46 Humayun et al., 1991; Jadoon, 1991; Jadoon et al., 1992; Jadoon et al., 1993; Jadoon et al., 1994;
47 Jadoon and Khurshid, 1996; Iqbal and Helmcke, 2004; Fitzsimmons et al., 2005; Shah, 2009;
48 Iqbal and Khan, 2012; Reynolds et al., 2015; Malkani et al., 2017; Khan, 2019a; Jadoon et al.,
49 2019). Nazeer et al. (2013) had carried out a synthesis of hydrocarbon potential of the Zindapir
50 Anticline using limited biostratigraphic from the Cretaceous intervals of the Zindapir-01 well
51 and geochemical data for source rock analysis. Detailed research in terms of seismostratigraphy
52 is scarce, with previous works mainly utilizing seismic reflection data to assess the geometries of
53 individual structures (e.g. Jadoon et al., 2019), hence limiting understanding of the wider setting
54 of the Sulaiman Basin.

55 The Sulaiman Fold-Thrust Belt is also a petroliferous tectonic region and an active area of
56 exploration wherein several exploratory wells have been drilled along with a number of 2D
57 seismic acquisition campaigns since the 1970s (see Table 1). Many significant hydrocarbon
58 discoveries are on record from a number of structural plays (including carbonate and clastics
59 petroleum plays of the Maastrichtian and the Paleogene age) in the south-western (e.g., Pirkoh
60 field) and northern parts (e.g., Dhodak field). The eastern part of the Sulaiman Fold-Thrust Belt
61 which includes the Foredeep, however, lacks significant discoveries in spite of robust
62 exploratory activities of different oil and gas companies in the region. To date, a large number of
63 exploratory wells have been drilled in the Foredeep area in search of hydrocarbons with
64 negligible success ratio.

65 We interpret major stratigraphic and lithologic variations in clastic/carbonate reservoir rocks
66 using seismic data, as well as new (seismic supported) regional tectono-stratigraphic models. The
67 research aims at producing a consistent regional model that honor the geological observations

68 from a wide region of the Sulaiman Basin: the Sulaiman Foredeep and the outer part (i.e. to the
69 east) of the Sulaiman Fold-Thrust Belt. Figure 1b shows the location of seismic lines and wells
70 used in this study. The model was constrained by seismic stratigraphic interpretation coupled
71 with seismic attribute analysis, tied with drill cuttings data from selected wells to understand
72 stratigraphic, lithological variations and tectono-stratigraphic influences. This paper is also an
73 attempt to shed new light on the reservoir-seal relationship, clastic-carbonate petroleum plays in
74 the Foredeep area and its comparison with the adjacent Sulaiman Fold-Thrust Belt (SFTB) and
75 the Zindapir Anticline.

76

77 **2. Background and Geological Setting**

78 In the northwestern and western Pakistan, the formation of the Sulaiman and Kirthar Ranges is
79 the result of oblique collision of the Indian Plate with the Eurasian Plate in a transpressional zone
80 (DeJong and Farah, 1979; Lawrence et al., 1981; Farah et al., 1984; Quittmeyer and Kafka,
81 1984; Jadoon et al., 1992, 1994; Jadoon and Khurshid, 1996). This is part of the wider
82 Himalayan collision zone marked in the North by the Main Mantle Thrust and to the West by the
83 Chaman Fault (Fig. 1a). The relative plate motion of the Indian Plate towards the NW is
84 accommodated by the Chaman Fault, forming a transpressional boundary zone (Jacob and
85 Quittmeyer, 1979) as well as by thrust faulting in the Sulaiman Fold-Thrust Belt to the southeast
86 (Bernard et al., 2000; Szeliga et al., 2012). Local strike-slip faults are thought to interact with the
87 larger contractional structures of the Sulaiman Fold-Thrust Belt – e.g. Kingri, Fault (Rowlands,
88 1978; Humayun et al., 1991; Bernard et al., 2000). The Sulaiman Range, referred to as the
89 Sulaiman Basin in this study, lies to the north of the Kirthar Range (Banks and Warburton, 1986)

90 and between the Katwaz basin to the west and the Sulaiman Foredeep and Punjab platform to the
91 east (Fig. 1).

92 The basin evolution in the study area started during the Paleogene as a response to subduction of
93 the Indian Plate beneath the Eurasian Plate. The basin architecture and evolution were further
94 shaped by the influence of tectonics from the Afghan Block in the west during the Tertiary
95 (Treloar and Izzat, 1993). The structural orientation in the southern Sulaiman Basin is east-west,
96 whereas the eastern and northern Sulaiman regions are dominated by north-south trending
97 structures comprising thrust faults, asymmetrical folds as delineated from the seismic reflection
98 profiles. To the east of the Sulaiman Fold-Thrust Belt is the Foredeep region, wherein the
99 possibility of stratigraphic plays is expected.

100

101 The constant motion of the Indian Plate in the extreme north, where the Indian Plate is subducted
102 beneath the Eurasian Plate, and the interaction of the Indian Plate with Afghan Block in the
103 northwest Sulaiman Fold-Thrust Belt suggest the likely repeated activation of folds and faults in
104 this region. Reynolds et al. (2015) in their work present observations and models of the western
105 Sulaiman Range (Pakistan) describing the evolution and deformation of fold-thrust belts.
106 Structurally, the Sulaiman Lobe marks the southern end of the Sulaiman Fold-Thrust Belt, which
107 is interpreted to have evolved as a thin-skinned feature over a weak decoupling zone (Davis and
108 Engelder, 1985; Jadoon, 1991; Jadoon et al., 1992; 1993; 1994). The amount of shortening in the
109 Sulaiman Fold-Thrust Belt represents about 50% of the average plate convergence rate of about
110 37 mm/yr between the Indian Plate and the Afghan Block (Minster et al, 1974; Minster and
111 Jordan, 1978; Jacob and Quittmeyer, 1979). Continental basement is not found to be involved in
112 the deformation in the Sulaiman Fold-Thrust Belt, and the left-lateral strike-slip Chaman fault

113 system in the west is known to be accommodating shortening (Jadoon, 1991; Jadoon et al., 1992;
114 1993).

115
116 From a stratigraphic standpoint, the Jurassic sequence is composed of limestone and shales, that
117 were deposited in a pre-collisional setting in the region, at a time when the Neo-Tethys Ocean
118 separated the Afghan Block from the Indian Plate (Fig. 2). The Cretaceous units also represent
119 pre-collision deposits forming the westward sloping shelf of the Indian Plate (Sultan, 1997). The
120 dominant Cretaceous units are shelf carbonate deposits (Parh Formation) or near-shore clastic
121 deposits (Mughal Kot Formation); however, channel deposits are present in the upper Cretaceous
122 Pab Formation (Khan and Clyde, 2013) (Fig. 2). The Pab Sandstone and Mughal Kot Formation
123 are the dominant Cretaceous successions, while Parh Formation and Goru-Sembar successions of
124 the Cretaceous are only encountered in three wells (Burzi-01, Zindapir-01 and Sakhi Sarwar-01).
125 The Neocomian (Early Cretaceous) Sembar Shale is a proven source rock in the area (Fig. 2).

126
127 The emplacement of the Muslimbagh Ophiolites over the Cretaceous shelf sediments during the
128 Paleocene to early Eocene is thought to mark the initiation of a collisional sequence made of
129 shallow marine units (Fig. 2; Khan and Clyde, 2013). The Paleocene units drilled in the study
130 area include the Dunghan and Ranikot formations of Ranikot Group, and the Eocene Kirthar
131 Group including the Habib Rahi Limestone, Sirki-Domanda Shale, Pirkoh Limestone and
132 Drazinda Formation. The Miocene-Pliocene rock units, including Chinji, Gaj, and Nari comprise
133 the Siwaliks Group in the Sulaiman Foredeep area and represent a continuous parallel to
134 subparallel reflection bedding configuration, with medium frequency and medium to high

135 amplitude. These depositional sequences are inferred as fluvial/deltaic clastics (Flynn, 1972;
136 Shah, 2009; Malkani, 2017).

137 **3. Methods**

138 The seismic interpretation focused essentially on the clastics and carbonate rocks of the
139 Cretaceous and Paleogene, including the Neogene strata from the Zindapir Anticline and the
140 Foredeep. Seismic horizons and key faults were picked using 2D time-migrated seismic data
141 released by the Directorate General of Petroleum Concession (DGPC) (see Table 1 and Fig. 1b).
142 Data quality was varied and generally low for the lines covering the Dhodak near the Zindapir
143 Anticline. There were extensive mis-ties among the seismic stratigraphic horizons during
144 interpretation that were corrected by employing mis-tie analysis. The interpretation was aided by
145 the use of instantaneous phase seismic attribute, to highlight the continuity of reflections and
146 stratal terminations. Interpretation of seismic data and calculation of seismic attributes was done
147 in IHS Kingdom software. The instantaneous phase was calculated as:

$$148 \quad Ph(z) = \frac{180}{\pi} \operatorname{arc} \tan \left[\frac{g(z)}{f(z)} \right] \quad 1$$

149 where z is either time or depth, $f(z)$ and $g(z)$ are the real and imaginary components of the
150 complex trace described for the imaginary part attribute $g(z)$, which is in turn computed through
151 the Hilbert transform of the real part.

152 Interpretation of each line proceeded from well-imaged, well-constrained portions of the line
153 toward areas of poorer constraint. The polarity of seismic data is zero phase with the usage of the
154 American polarity i.e., positive polarity (impedance) is linked to a peak (positive amplitude). The
155 vertical seismic resolution was calculated using dominant frequency and velocities from well
156 data. This falls in the range of 20– 50 m for the seismic lines in the south and 25– 40 m for those

157 in the north. Line spacing is highly variable as seen in Figure 1. To the north, around the
158 Dhodak-05, line spacing is ~30 km, whereas to the south, near the Choti-1 well, it is in the range
159 of 50–150 km.

160 A Ricker wavelet of 25 Hz frequency was selected to generate synthetic seismic data by
161 convolving the reflectivity derived from digitized acoustic (DT) and density (RHOB) logs with
162 the wavelet derived from seismic data. This was implemented to tie seismic data with eight wells
163 and wireline logs used for stratigraphic correlation. Electrical logs such as gamma ray-neutron
164 log (GR-NPHI), sonic log (DT) and density (RHOB) were used for correlation between wells.
165 The time-depth charts were generated using the sonic log (DT) and density (RHOB) data, since
166 vertical seismic profile (VSP) and check shots (CS) survey were either not available for certain
167 wells, or were not in the public domain to be used for research purpose. The established time-
168 depth (T-D) tables were used to tie the wells to the seismic data and derive two-way travel time
169 (TWT) information. In order to tie-in the well results with seismic referred to as seismic
170 calibration with well data, synthetic seismogram or trace were generated for selected wells.

171 Besides analyzing the electrical logs of exploratory wells to aid in seismic interpretation,
172 microscopic studies of drill cuttings from two selected wells were performed using a polarizing
173 microscope with an image-capturing system. The main objective was to identify lithology and
174 extract faunal information in order to tie well data with seismic for erecting tectono-stratigraphic
175 models for the Cretaceous and Paleogene Periods and to derive climatic implications and
176 depositional scenarios for this time period. The two types of microscopic examination performed
177 to study drill cuttings included: (a) reflected light for whole fossil examination e.g. foraminifera
178 where surface features are recognized under low magnifications, and (b) transmitted light to
179 study litho-biofacies in thin sections for higher-powered magnifications. Time-depth charts

180 (Appendix-A) indicate the seismic to well tie for correlation, whereas, a flow diagram
181 (Appendix-B) explains our approach carried out for seismic stratigraphic and structural
182 interpretations.

183 **4. Results**

184 **4.1. Litho-biofacies**

185 Seismic stratigraphy was derived for Choti-01 from the Sulaiman Foredeep domain (Fig. 3a) and
186 drill cuttings from two wells (Zindapir-01 and Burzi-01) were studied for litho-bio information
187 (Fig. 3b and 3c). In Fig. 3a, the key seismic horizons interpreted are the Neogene (Chinji [1121
188 m], Gaj-Nari [757 m]) and the Paleogene (Drazinda, Dunghan). Seismic stratigraphy results
189 indicate the Neogene sediments show parallel, continuous medium to high amplitude reflection
190 patterns. The Eocene Drazinda Shale (192 m in Choti-01) appears to act as a detachment level
191 for the younger Neogene folds in the Foredeep area (Fig. 3a). The Eocene Pirkoh unit is 16 m
192 thick in the Choti-01 whereas the Paleogene sediments (Dunghan) drilled thickness is around 16
193 m. The Eocene detachment Ghazij Shale has a drilled thickness of 413 m in Choti-01 of the
194 Sulaiman Foredeep. Figures 3b and 3c show the presence of abundant planktonic foraminifera in
195 the Cretaceous (Parh Formation) and Paleocene (Dunghan, Upper Ranikot) strata. Glauconite is
196 also observed in both the Cretaceous and Paleocene successions, notably in the Cretaceous Goru
197 (representing clastics with alternating shale) and carbonates of the Paleocene Epoch (i.e.,
198 Dunghan and Upper Ranikot) (Figs. 3b–c).

199

200 Stratigraphically, the major units in the area include the Cretaceous (Aptian-Albian) Goru
201 Formation, Campanian Parh Limestone, late Campanian to Maastrichtian Mughal Kot and the

202 Maastrichtian Pab Sandstone. The Goru and Pab sequences are proven petroleum system
203 reservoirs in the Central and Lower Indus Basins of Pakistan. The reservoir potential of the
204 Mughal Kot unit appears as secondary whereas no petroleum accumulations have been reported
205 from the Campanian Parh Formation so far. The middle Eocene Habib Rahi Limestone is a
206 secondary reservoir target in some fields of the Central Indus Basin (Pakistan), however, in the
207 study area, there is not enough dataset available that can shed light on the petroleum assessment
208 of the Habib Rahi Limestone (49 m drilled thickness in the Choti-01). The drilled thickness of
209 the Sembar Shale, which is a source rock in the area is 757 m in the Zindapir-01 well.

210
211 In Figs. 3b and 3c, the Cretaceous (Aptian-Albian) Goru unit indicate coarsening upward trend at
212 alternate intervals indicative of sand packages within Goru shale sequence (527 m thick in the
213 Burzi-01 and 296 m in the Zindapir-01), coarsening upward, increase in depositional energy
214 whereas fining upward, decrease in depositional energy. The Campanian Parh limestone in the
215 Burzi-01 (206 m) and the Zindapir-01 (91 m) illustrate straight constant gamma ray trends with
216 aggrading geometry and no significant variation in facies. The gamma ray motif also shows the
217 negligible argillaceous content. The Campanian to Maastrichtian Mughal Kot unit (19 m thick in
218 the Burzi-01 to the west and 407 m thick in the Zindapir-01) indicates a rather regular gamma
219 ray signature representing aggrading sands or silt in both wells (Figs. 3b and 3c). The
220 Maastrichtian Pab Sandstone (880 m thick in the Burzi-01 and 428 m in the Zindapir-01) shows
221 repeated fining and coarsening upward stacking patterns indicating alternating transgressive-
222 regressive (T-R) cycles. The Paleocene unit Ranikot is 120 m in the Burzi-01 and 88 m in the
223 Zindapir-01 whereas the Dunghan Formation is only encountered in the Zindapir-01 with 100 m

224 thickness. The middle Eocene Habib Rahi Limestone is only encountered in the Choti-01 and
225 indicates a nearly cylindrical trend suggesting aggrading carbonate shelf margin.

226

227 **4.2. Seismostratigraphic Interpretation**

228

229 **4.2.1. Zindapir Anticline area**

230 Seismic data in the northern end of the Zindapir Anticline show anticlinal structures and reverse
231 faults dominantly oriented NW and NE directions (Figs. 4 and 5). Here, discontinuous reflections
232 are dominant likely due to structural disturbances and imaging issues of structurally complex
233 terrains. The folds are largely symmetric and detach at depth within the subparallel Cretaceous
234 strata – probably the Sembar Shale. The Eocene strata appear to be folded and truncated at the
235 surface. This evidence together with the lack of obvious growth strata in the Cretaceous and
236 Paleocene section indicates a post-Eocene folding. Parasitic deformation associated with the
237 main anticline is observed as small scale detachment folds and fault propagation folds affecting
238 the Eocene strata. These structures were likely accommodated by the presence of a weak
239 detachment in the Ghazij Shale.

240 Folds from the Zindapir Anticline are analyzed using the fold wavelength vs. thickness graph
241 from Morley et al. (2011). We used the stratigraphic thickness for competent lithology with shale
242 detachment. The folds from the Zindapir Anticline domain are compared with other examples of
243 the fold and thrust belts (FTBs') from around the world. The Makran region of Iran and Pakistan
244 is also included for comparison with the study area. The graph indicates fold wavelengths of
245 around 10-14 km attributed to thin-skinned deformation, with relatively less sedimentary
246 thickness in contrast to the Zagros FTB Iran. The fold amplitude and wavelength is more related

247 thickness of the sedimentary section rather than the FTB type (Morley et al., 2011). In
248 comparison to salt detachment FTBs, shale detachment FTBs display fewer detachment folds,
249 less variation in vergence and short duration of deformation (Morley et al., 2011). In comparison
250 to other deep-water FTBs worldwide examples (Fig. 6), the Sulaiman Fold-Thrust Belt (SFTB)-
251 Zindapir Anticline (ZA) does not indicate the very large volume of sediment deposition in the
252 basin most probably due to continuous cycles of uplifting and erosion as indicated from the work
253 of Khan (2019a). Unlike the Sulaiman Fold-Thrust Belt (SFTB)-Zindapir Anticline (ZA)
254 (Pakistan), the two largest wavelength provinces (South Caspian Sea, Zagros Mountains) are
255 associated with 10 km+ thickness of sedimentary rock overlying the salt detachment (Morley et
256 al., 2011).

257 ***4.2.2. Sulaiman Foredeep area***

258 As shown in Figures 7, 8 and 9, structurally, the Sulaiman Foredeep domain is characterized as a
259 west-dipping monocline wherein the presence of the Neogene folds and the Paleogene
260 stratigraphic thickening near the Drazinda interval is evident. The high continuity of reflections
261 in the younger strata suggests a great lateral extent of the same sedimentation conditions (Figs.
262 7–8) and the parallel nature of the reflections indicates deposition in a rather stable depositional
263 environment. In places, prominent clinofold units likely document prograding shelf slope
264 systems during the Eocene (Fig. 9). These systems are 13 km across and their occurrence can be
265 translated in terms of depositional environments i.e., from a sand-prone shelf (proximal to the
266 east) into a shale-prone slope (finer-grained) and ending up in the shale-prone basinal
267 environment (distal portion to the west). Within the Eocene, the prograding units may represent
268 novel traps for hydrocarbon exploration in the Sulaiman Foredeep.

269 Stratigraphic thickness expansion was identified on seismic lines FZP-06 and FZP-12 (Figs. 7
270 and 8). The seismic reflection profile 954-FZP-12, at TWT of 2.4–2.7 sec indicates the presence
271 of development of stratigraphic thickness expansion (Fig. 9a and b). These form divergent
272 reflections fanning towards the west for a length in excess of 1–4 km. It is observed that the base
273 of the expansion is not erosional in nature, indicating that the thickness variation might be
274 tectonic and not due to sedimentary infill. This, together with the fact that units immediately
275 above and below the thickness expansion are parallel (Fig. 8), indicate that this feature developed
276 as a result of a major phase of basin subsidence to the west of the Sulaiman Foredeep.

277 Gentle folds 1–10 km across are observed to affect the Paleogene-Neogene strata to the western
278 portion of the Sulaiman Foredeep (Fig. 5). This is evidenced by the Neogene and recent strata
279 folded and eroded at the ground level. Imaging at depth is challenging, however, planar packages
280 of reflections in the Lower Eocene and the Upper Cretaceous section would indicate the presence
281 of a detachment surface for the Neogene folds at that level. Folding of these strata does not
282 exhibit evidence of clear growth strata, indicating a recent phase of deformation.

283 **5. Discussion**

284 **5.1. Sulaiman Fold-Thrust Belt tectono-stratigraphic evolution**

285 Figures 10–12 illustrate the tectono-stratigraphic architecture of the study area during the
286 Cretaceous-Paleogene and Present-day based on the results and interpretations of this work. The
287 models demonstrate the tectonic evolution of the eastern Sulaiman Fold-Thrust Belt and the
288 Foredeep progression and the associated variations in basin-fill stratigraphy and stratal
289 architecture. As indicated from the litho-biofacies analysis, the Late Cretaceous (Parh
290 Limestone) shows abundant planktonic foraminifera suggesting late transgressive and early

291 highstand evidencing sea level rise during this period. The glauconite presence in the Cretaceous
292 strata also suggests shelfal to shallow marine environments with low sedimentation rates, adding
293 evidence to an overall transgression at this time. In the Late Cretaceous (Fig. 10), the study area
294 was characterized by shallow seas and prevailing deltaic and shallow marine environments with
295 the terrigenous influx from the east. This has also been documented from the paleogeographical
296 works of Flynn (1972), Shah (2009) and Khan (2020) across the northwest Indian Plate (East
297 Gondwana fragment). The Cretaceous also evidenced the development of shoal area (Flynn,
298 1972) with sandbanks and bars to the west of the area (Fig. 10). The Maastrichtian Pab
299 Sandstone and the Campanian to Maastrichtian Mughal Kot are also of fluvio-deltaic and
300 shallow marine origin (Malkani, 2010).

301 The importance of glauconite in deciphering depositional environments has been extensively
302 discussed in literature (Porrenga, 1967; Amorosi, 1997; Jiménez-Millan et al., 1998; Kelly and
303 Webb, 1999; Lim et al., 2000; Bansal et al., 2018; Khan, 2019b) and the mineral is known to
304 have been associated with stratigraphic strata deposited in continental and shelfal, shallow
305 marine environments with low sedimentation rates. Describing the interpretation of litho-
306 biofacies results, the occurrence of glauconite suggests that the Cretaceous and Paleocene strata
307 in the Sulaiman Fold-Thrust Belt and the adjacent Foredeep witnessed rather low-moderate
308 temperatures (i.e. $< 15^{\circ}\text{C}$) and late transgressive accompanied by maximum flooding surfaces to
309 early highstand system tracts characterizing sea level rise during the Paleocene. The presence of
310 abundant planktonic foraminifera also endorses the above assumption since planktonics are
311 known to occur abundantly in late transgressive and early highstand evidencing sea level rise
312 (Emery and Myers, 1996; Fung et al., 2019; Khan, 2020).

313 During the Paleogene (Fig. 11), it is proposed that due to ongoing collision to the west, orogenic
314 loading caused crustal flexure developing in the Foredeep, in front of the incipient Sulaiman
315 Fold-Thrust Belt. Figure 8 is a zoomed image extracted from the seismic reflection profile (Fig.
316 7) showing a detail section of the stratigraphic thickness expansion. This change in thickness is
317 not an infill of an erosional feature since there is no evidence of erosion on seismic record, but
318 likely due to changes in accommodation space driven by flexure from the west. The creation of
319 accommodation at this time is also indicated by prograding units and clear stratigraphic thickness
320 expansion causing bed thickening towards the west observed along other seismic line (Figs. 7, 8
321 and 9; seismic lines 954-FZP-06 and 954-FZP-12 of the Choti-01). The ages of stratigraphic
322 thickness expansion in the Sulaiman Foredeep domain may indicate the timing of collision and
323 crustal flexure, which is the Paleogene. As collision initiated to the west, deformation
324 progressively propagated to the east as shown by folding observed in the Zindapir Anticline
325 region (Figs. 4 and 5). Here, folding and uplift together with the lack of strata younger than the
326 Eocene, suggest that the deformation front reached the area around that time.

327 In the Neogene to present day, the orogenic front reached the Sulaiman Foredeep as indicated by
328 the presence of Neogene folds here (Figs. 7 and 12). Additional evidence of potential progressive
329 deformation towards the east is provided by the occurrence of well-developed, symmetric
330 detachment folds observed in the Zindapir Anticline area (Fig. 4 and 5) which contrasts with the
331 gentle folds affecting the shallow section of the Sulaiman Foredeep to the east. Progressive
332 deformation to the east during the Paleogene in the Sulaiman Fold-Thrust Belt is supported by
333 field work data from Wang et al. (1996) and seismologic and neotectonics analysis from Baig et
334 al. (2002). Wang et al. (1996) documented the development of a large shear zone in the region
335 associated with transform/wrench faults and progressive initiation of a foredeep basin.

336 The investigation also indicates the presence of multiple detachments operating in the Sulaiman
337 Fold-Thrust Belt (Fig. 12). A deep, Cretaceous detachment is suggested to exist and
338 accommodate the formation of major folds in the Zindapir Anticline area (Fig. 4 and 5). The
339 Sembar Shale of Neocomian age as seen in Figure 3c, which is dominantly shale unit, maybe a
340 good candidate for such decollement. A shallower detachment is also required to accommodate
341 the pervasive deformation associated with the main folds affecting the shallow Eocene strata
342 (Figs. 4 and 5). This detachment probably within the Ghazij Shale of the Eocene age, is widely
343 extensive as seems to control the Neogene folds observed further east, in the Sulaiman Foredeep
344 (Fig. 7). The occurrence and involvement of these weak layers in the deformation were key in
345 shaping the structural styles of the Sulaiman Fold-Thrust Belt (Fig. 12). A similar set of potential
346 mechanically weak units in the Lower Cretaceous and Eocene is reported by Jadoon et al.
347 (2019).

348 The presence of multiple detachments within the thrust belts in the Himalayan and Ouachita
349 (southern United States) examples indicate that the formation of an intermediate-level
350 detachment and the deposition of foreland basin sediments are temporally related to the same
351 orogenic event (Chapman and DeCelles, 2015). Multi detachment patterns are also reported from
352 the Canadian Rocky Mountains in the Middle Cretaceous Alberta Group and Upper Cretaceous
353 Bearpaw Formation (Spratt and Lawton, 1996) and the Swiss Central Jura associated with thin-
354 skinned deformation (Schori et al., 2015). Basal detachment corresponding to shale within the
355 Lower Eocene has been documented from the port Isabel Fold Belt of the western Gulf of
356 Mexico, where shale detachments at shallower levels have been described (Peel et al., 1995).
357 Similarly, the Neocomian Sembar Shale and the Eocene Ghazij Shale have been critical for the
358 development of the detachments observed in the study area.

359 The stratigraphic thickness expansion such as the one observed in the Sulaiman Foredeep is
360 typical of foredeep depozones and results from the flexural subsidence caused due to
361 topographic, sediment and subduction loads (DeCelles and Giles, 1996). The propagation of
362 deformation from west to the east and rapid filling of foreland basin as observed in the SFTB-ZA
363 and the Foredeep shows similarity to the North Alpine Foreland Basin of France and
364 Switzerland, where an increase in foreland sedimentation is well documented (Erdős et al.,
365 2019). The increase in sedimentation and the onlap of sediments onto the foreland has been
366 extensively described in the North Alpine Foreland Basin (e.g., Sinclair, 1997; Erdős et al.,
367 2019). The thickness expansion as observed in the Sulaiman Foredeep is further supported by the
368 point that the growth of orogen results in surface areas with higher elevation, an increase in
369 erosion rates and subsequently sediment flux into the Foreland basin (Simpson, 2006a; Sinclair et
370 al., 2005). A prime example, may be the southern Pyrenean (pro-) Foreland fold and thrust belt,
371 indicating middle Eocene increase in sedimentation rate (Sinclair et al., 2005) similar to the
372 middle Eocene from the Sulaiman Foredeep.

373 The sediment accumulation rate in the foredeep depozone increases rapidly toward the orogenic
374 wedge (Sinclair et al., 1991; Flemings and Jordan, 1989) and these foredeep sediments are
375 dominantly derived from the fold-thrust belts (Schwab, 1986; DeCelles and Hertel, 1989; Critelli
376 and Ingersoll, 1994). The seismic record does not reveal any significant unconformities probably
377 due to the high rates of subsidence and sediment supply associated with crustal thickening and
378 orogenic loading (e.g., Fleming and Jordan, 1989; Coakley and Watts, 1991; Sinclair et al.,
379 1991). As observed in the Sulaiman Foredeep, characterized by sediment deposited between the
380 structural front of the fold thrust belt and the forebulge, the sediment thickness increases toward
381 the front of the thrust belt (DeCelles and Giles, 1996).

382 The flexure and uplift of the Sulaiman Fold-Thrust Belt is documented to be related to early and
383 late Tertiary inversion of extensional and transtensional basins along the northwest margins of
384 the Indian continental plate (Treloar and Izatt, 1993). Since the Paleocene, uplift and
385 compression in the region have been episodic, however, the main phase of compression and
386 uplift was during the Pliocene to the present (Khan et al., 2012). According to Khan and Clyde
387 (2013), the Sulaiman Basin is a part of the Indus Basin, a northeast trending foreland basin
388 bounded by tectonic uplifts to the north and west and in the southeast lies the Indian craton. The
389 Indian craton is further traversed by a number of basement highs (Sargodha and Jacobabad
390 highs) (see Fig. 12). The tectonic movements such as uplift or subsidence of the lithosphere can
391 cause changes in sea level. Progradation or formation of prograding units may be due to the
392 growth of river delta further out into the sea and likely caused due to sea level fall resulting in
393 marine regression.

394 In many modern examples worldwide (Zagros, Himalayan, Taranaki, Andean, Apennine,
395 Taiwan, north Australian), four-part division of the foreland basin systems exists, however,
396 important distinctions in stratigraphic records among different foreland tectonic settings have
397 been revealed (Sinclair, 1997). Many foreland basin systems worldwide are characterized by a
398 wedge-top, foredeep, forebulge and backbulge depozones districting scheme (DeCelles, 2012).
399 Foredeep deposits are known to occur between the forebulge disconformity and wedge-top
400 deposits. Coarse-grained proximal facies with growth structures are reported from foreland basin
401 depo-zones (DeCelles, 2012). Our findings cover the wedge-top and foredeep deposits whereas
402 no forebulge and backbulge depozones could be studied due to nonavailability of seismic data.
403 Because of their structural elevation, the wedge-top deposits are vulnerable to erosion, and the
404 preservation of backbulge and forebulge deposits depends in part on tectonic setting (DeCelles,

405 2012). The seismic record in this study reveals that the Neogene-Recent strata from the SFTB-
406 ZA are eroded (see Figs. 4 and 5). The Sulaiman Foredeep depozone characterizes sediment
407 deposited within the flexural trough (Price, 1973) formed due to the load of the thrust belt (see
408 Figs. 7, 8 and 9).

409 **5.2. Implications for hydrocarbon exploration**

410 Figure 13 illustrates a diagrammatic play cross-section across the SFTB-ZA and the Foredeep
411 compiled from this study showing the seismic stratigraphy results derived from this research and
412 major petroleum system elements. Based on our interpretations, the broad folds and prograding
413 units in the Foredeep and thrust ramps at depth in the Zindapir Anticline may serve as new
414 potential exploration plays. The total petroleum system or petroleum play in the area includes the
415 following components: The Lower Cretaceous Sembar Formation represents the source, the
416 Upper Cretaceous (Pab, Mughal Kot), the Paleocene formations (Ranikot [proven], the Dunghan
417 [probable]) and the Eocene formations (Pirkoh, Habib Rahi Limestone) are reservoir rocks (Figs.
418 2 and 12), while a regionally extensive cap rock is present in the form of the Ghazij Group (Fig.
419 2). The formation of traps in the area is attributed to the Himalayan orogeny, whereas maturation
420 of source rock and migration pathways is related to burial and structuration during the Neogene.

421 Due to the complex tectonic setup of the region, the petroleum exploration plays of the Sulaiman
422 Fold-Thrust Belt and the Foredeep are varied. While most of the accumulations seem to be in the
423 foreland and foothills region, Paleogene shelf sediments in topsets from the Foredeep may act as
424 new exploratory plays. In the Foredeep, however, there might be issues with seal or trapping
425 mechanism to be less effective, in contrast to the fold belt in the west where the traps are mainly

426 thrust folds. The hydrocarbon accumulation in the east appears to be less preserved, possibly due
427 to tectonism in the west.

428 The petroleum system investigation in the study area based on our results implies variable
429 reservoirs, and most likely seal issues within petroleum system elements notably to the east. The
430 development of high pressure across different lithologies particularly shales and in some cases
431 carbonates/clastics may likely be evidence of seal breaching. Here one reason for seal breaching
432 may be attributed to lithological contrast across different reservoir compartments. A positive
433 shift/change in pressure characterizes a competent seal, whereas, negative change may reflect
434 seal breach due to a structural failure such as fault, salt interface, high pressured shales, and/or an
435 unconformity. The varied structural and stratigraphic features developed through the late
436 Cretaceous, the Paleogene and the Neogene history of the basin offers high-trapping potentials
437 for a number of clastic and carbonate plays.

438 **6. Conclusions**

439 Our analysis of seismic and well data provides new constraints for the tectono-stratigraphic
440 evolution of the Sulaiman Fold-Thrust Belt and the Sulaiman Foredeep through the Cretaceous
441 and present-day. The main conclusions of this research are summarized as follows:

- 442 • The Sulaiman Fold-Thrust Belt forms a thin-skinned system of well-developed
443 detachment folds, 2-14 km, with the Sembar Shale of Neocomian age operating as the
444 main decollement unit. The folds affect 2 km of Paleogene-Eocene strata, with the
445 Eocene Ghazij Shale accommodating small scale, parasitic folding on the limbs of the
446 main structures.

- 447 • Evidence for an overall eastward migration of deformation is given by the presence in the
448 Sulaiman Foredeep of much bland structuration in the form of gentle folds detaching
449 above the Eocene decollement and affecting the Neogene to recent succession. Here,
450 thickness expansion of the Paleogene stratigraphy provided evidence of a phase of
451 accelerated subsidence likely linked to crustal flexure.
- 452 • Further evidence of initial contractional crustal load, flexure and basin development in
453 the hinterland of the Sulaiman Fold-Thrust Belt during the Paleogene is given by clear
454 imaging of same age prograding shallow marine units into deeper water to the west.
- 455 • Thrust ramps in the Zindapir Anticline, Paleogene shelf sediments (most probably the
456 Dughan and the Habib Rahi Limestone) in topsets from the Sulaiman Foredeep may act
457 as new exploratory plays along with clastic sediments. In the Sulaiman Foredeep,
458 however, there might be issues with seal or trapping mechanism to be less effective in
459 contrast to the fold belt in the west where the traps are mainly simple detachment folds.
- 460 • The socio-economic benefit of resource investigations suggests that the quest for new
461 petroleum plays in the area will act as a catalyst for research and exploration in this
462 petroliferous sedimentary basin.

463 **Acknowledgments**

464 The Directorate General of Petroleum Concessions (DGPC) and Hydrocarbon Development
465 Institute of Pakistan (HDIP), Islamabad, Pakistan, are gratefully acknowledged for releasing
466 seismic and well data for this research and permission to publish the work. We are thankful to
467 the Department of Earth Sciences, Royal Holloway University of London, Egham, UK, for
468 providing research facilities. We thank two anonymous reviewers for the constructive comments

469 to improve the manuscript. The Editor in Chief of JAES, Prof. Mei-Fu Zhou and **Dr. Vineet**
470 **Gahalaut** are thanked for editorial handling and helpful suggestions.

471

472 **References**

473 Amorosi, A., 1997. Detecting compositional, spatial, and temporal attributes of glaucony: a tool
474 for provenance research. **Sedimentary Geology**, 109, 135–153.

475

476 Baig, M.A.S., Mazhar, F., Rahman, M.U., Mehmood, H., 2002. Seismotectonic set up in East
477 Central Sulaiman Range. *Geological Bulletin, University of Peshawar*, 35, 67–84.

478

479 Banks, C.J., Warburton, J., 1986. “Passive-roof” duplex geometry in the frontal structures of the
480 Kirthar and Sulaiman mountain belts, Pakistan. *Journal of Structural Geology*, 8, 229–237.

481

482 Bansal, U., Banerjee, S., Ruidas, D.H., 2018. Compositional evolution of glauconite within the
483 Upper Cretaceous Bagh Group of sediments, India. *Geophysical Research Abstracts*, 20,
484 EGU2018-1677, EGU General Assembly.

485

486 Bernard, M., Shen-Tu, B., Holt, W.E., Davis, D.M., 2000. Kinematics of active deformation in
487 the Sulaiman Lobe and Range, Pakistan. **Journal of Geophysical Research**, 105, 13253–13279.

488

489 Coakley, B.J., Watts, A.B., 1991. Tectonic controls on the development of unconformities: The
490 North Slope, Alaska. *Tectonics*, 10, 101–130.

491

492 Crawford, A.R., 1974. The Salt Range, the Kashmir Syntaxis and the Pamir Arc. Earth and
493 Planetary Science Letters, 22, 371–379.

494 Critelli, S., Ingersoll, R.V., 1994. Sandstone petrology and provenance of the Siwalik Group
495 (northwestern Pakistan and western-southeastern Nepal). *Journal of Sedimentary Research*, 64,
496 815–823.

497 Davis, D., Engelder, T., 1985. The role of salt in fold-and-thrust belts. *Tectonophysics*, 119, 67–
498 88.

499 DeCelles, P.G., Hertel, F., 1989. Petrology of fluvial sands from the Amazonian foreland basin,
500 Peru and Bolivia. *Geological Society of America Bulletin*, 101, 1552–1562.

501 DeCelles, P.G., Giles, K.A., 1996. Foreland basin systems. *Basin Research*, 8, 105–123.

502 DeCelles, P.G., 2012. Foreland basin systems revisited: variations in response to tectonic
503 settings. In: *Tectonics of Sedimentary Basins: Recent Advances (First Edition)*, Edited by Cathy
504 Busby and Antonio Azor Pe ´rez. © 2012 Blackwell Publishing Ltd., 405–426.

505 DeJong, K.A., Farah, A., 1979. *Geodynamics of Pakistan*, Geological Survey of Pakistan Quetta,
506 362 pp.

507

508 Emery, D., Myers, K., 1996. *Sequence stratigraphy*. Blackwell Science Ltd., 297 pp.

509 Erdˆos, Z., Huismans, R.S., Peter vander Beek, P.V., 2019. Control of increased sedimentation
510 on orogenic fold-and-thrust belt structure–insights into the evolution of the Western Alps. *Solid*
511 *Earth*, 10, 391–404.

512 Farah, A., Abbas, G., DeJong, K.A., Lawrence, R.D., 1984. Evolution of the lithosphere in
513 Pakistan. *Tectonophysics*, 105, 207–227.

514 Fitzsimmons, R., Buchanan, J., Izatt, C., 2005. The role of outcrop geology in predicting
515 reservoir presence in the Cretaceous and Paleocene successions of the Sulaiman Range, Pakistan.
516 *AAPG Bulletin*, 89, 231–254.

517 Flemings, P.B., Jordan, T.E., 1989. A synthetic stratigraphic model of foreland basin
518 development. *Journal of Geophysical Research*, 94, 3851–3866.

519 Flynn, S.C., 1972. Post Permian stratigraphy and interpreted correlation of part of Northern and
520 Central Pakistan. Pakistan Geological Report, Unpublished AMOCO Exploration Company
521 Islamabad.

522 Fung, M.K., Katz, M.E., Miller, K.G., Browning, J.V., Rosenthal, Y., 2019. Sequence
523 stratigraphy, micropaleontology, and foraminiferal geochemistry, Bass River, New Jersey
524 paleoshelf, USA: Implications for Eocene ice-volume changes. *Geosphere*, 15, 502–532.
525

526 Humayun, M., Lillie, R.J., Lawrence, R.D., 1991. Structural interpretation of eastern Sulaiman
527 foldbelt and foredeep, Pakistan. *Tectonics*, 10, 299–324.

528 Jacob, K.H., Quittmeyer, R.C., 1979. The Makran region of Pakistan and Iran: trench-arc system
529 with active plate subduction. In: A. Farah and K.A. DeJong (eds.), *Geodynamics of Pakistan:*
530 *Geological Survey of Pakistan, Quetta*, 305–318.

531 Iqbal, M., Helmcke, D., 2004. Geological interpretation of earth quakes data of Zinda Pir
532 anticlinorium, Sulaiman Fold Belt, Pakistan. *Pakistan Journal of Hydrocarbon Research*, 14, 41–
533 47.

534 Iqbal, M., Khan, M.R., 2012. Impact of Indo-Pakistan and Eurasian Plates collision in the
535 Sulaiman Fold Belt, Vol., 50575 Search and Discovery Article.

536 Jadoon, I.A.K., 1991. Thin-skinned tectonics on continent/ocean transitional crust. Sulaiman
537 Range, Pakistan. Ph.D. Thesis, Oregon State University, USA., 166 pp.

538 Jadoon, I.A.K., Lawrence, R., Lillie, R., 1992. Balanced and retrodeformed geological cross-
539 section from the Frontal Sulaiman Lobe, Pakistan: Duplex development in thick strata along the
540 western margin of the Indian Plate. In: McClay K.R. (eds.) *Thrust Tectonics*. Springer,
541 Dordrecht, 343–356.

542

543 Jadoon, I.A.K., Lawrence, R., Lillie, R., 1993. Evolution of foreland structures: An example
544 from the Sulaiman Thrust Lobe of Pakistan, southwest of the Himalayas. Geological Society,
545 London, Special Publications, 74, 589–602.

546

547 Jadoon, I.A.K., Lawrence, R.D., Lillie, R.J., 1994. Seismic data, geometry, evolution, and
548 shortening in the active Sulaiman fold-and-thrust belt of Pakistan, southwest of the Himalayas.
549 *AAPG Bulletin*, 78, 758–774.

550

551 Jadoon, I.A.K., Khurshid, A., 1996. Gravity and tectonic model across the Sulaiman Fold Belt
552 and the Chaman Fault Zone in western Pakistan and eastern Afghanistan. *Tectonophysics*, 254,
553 89–109.

554 Jadoon, I.A.K., Zaib, M.O., 2018. Tectonic map of Sulaiman Fold Belt: 1:500,000 scale.
555 COMSATS University Islamabad (Abbottabad Campus), Pakistan.
556
557 Jadoon, S.U.R.K., Ding, L., Jadoon, I.A.K., Baral, U., Qasim, M., Idrees, M., 2019.
558 Interpretation of the Eastern Sulaiman Fold-and-Thrust Belt, Pakistan: a passive roof duplex.
559 *Journal of Structural Geology*, 126, 231–244.
560
561 Kelly, J.C., Webb, J.A., 1999. The genesis of glaucony in the Oligo-Miocene Torquay Group,
562 southeastern Australia: petrographic and geochemical evidence. *Sedimentary Geology*, 125, 99–
563 114.
564
565 Khan, I.H., Clyde, W.C., 2013. Lower Paleogene Tectonostratigraphy of Balochistan:
566 Evidence for Time-Transgressive Late Paleocene-Early Eocene Uplift. *Geosciences*, 3, 466–
567 501.
568 Khan, M.R., Bhatti, M.A., Baitu, A.H., Sarwar, M.Z., 2012. Effect of mega-shear fractures /
569 strike slip faults on entrapment mechanism in Sulaiman Fold Belt, Pakistan. *Search and*
570 *Discovery Article #30229*.
571 Khan, N. 2019a. Tectonic geomorphology and structural architecture of eastern Sulaiman Fold
572 Thrust Belt (SFTB) and adjacent Sulaiman Foredeep (SF), northwest Pakistan. *Geomorphology*,
573 343, 145–167.
574 Khan, N., 2019b. Application of integrated clustering and petrophysical-microscopic methods for
575 facies determination of Campanian–Maastrichtian and Danian–Thanetian reservoirs: Constraints

576 for tectonostratigraphic influences on sedimentation across the NW Indian Plate margin. Journal
577 of Petroleum Science and Engineering, 180, 861–885.

578 Khan, N., 2020. Stratigraphic analysis of Cretaceous and Paleogene successions in the eastern
579 Sulaiman Depositional Province, D.G. Khan, Pakistan: Implications for hydrocarbon potential.
580 Unpublished PhD Dissertation, NCE in Geology, University of Peshawar, Pakistan.

581 Lawrence, R.D., Khan, S.H., Dejong, K.A., Farah, A., Yeats, R.S., 1981. Thrust and strike-slip
582 fault interaction along the Chaman Fault Zone, Pakistan, in K. R. McClay and N. J. Price, eds.,
583 Thrust and Nappe Tectonics: Geological Society of London Special Publication, 9, 363–370.

584 Lim, Dhong il., Park, Y.A., Choi, J.Y., Cho, J.W., Khim, B.K., 2000. Glauconite grains in
585 continental shelf sediments around the Korean Peninsula and their depositional conditions. Geo-
586 Marine Letters, 20, 80–86.

587 Malkani, S.M., 2010. Updated stratigraphy and mineral potential of Sulaiman Basin Pakistan.
588 *Sindh University Research Journal*, 42, 39–66.

589 Malkani, M.S., Mahmood, Z., Alyani, M.I., Shaikh, S.I., 2017. Revised stratigraphy and mineral
590 resources of Sulaiman Basin, Pakistan. Geological Survey of Pakistan, Information Release No.
591 1003, 65 pp.

592 Jiménez-Millan, J., Molina, J.M., Nieto, F., Nieto, L., Ortiz, P.A.R., 1998. Glauconite and
593 phosphate peloids in Mesozoic carbonate sediments (Eastern Subbetic Zone, Betic Cordilleras,
594 SE Spain). *Clay Minerals*, 33, 547–559.

595 Minster, J.B., Jordan, T.H., Molnar, P., Haines, E., 1974. Numerical modelling of instantaneous
596 plate tectonics. *Royal Astronomical Society Geophysics Journal*, 36, 541–576.

597 Minster, J.B., Jordan, T.H., 1978. Present day plate motions. *Journal of Geophysical Research*,
598 83, 5331–5354.

599 Morley, C.K., King, R., Hillis, R., Tingay, M., Backe, G., 2011. Deepwater fold and thrust belt
600 classification, tectonics, structure and hydrocarbon prospectivity: A review. *Earth-Science*
601 *Reviews*, 104, 41–91.

602

603 Nazeer A., Solangi, S.H., Brohi, I.A., Usmani, P., Napar, L.D., Janhangir, M., Hameed, S., Ali,
604 S.M., 2013. Hydrocarbon potential of Zinda Pir Anticline, eastern Sulaiman Fold Belt, Middle
605 Indus Basin, Pakistan. *Pakistan Journal of Hydrocarbon Research*, 22–23, 73–84.

606

607 *Peel, F.J., Travis, C.J., Hossack, J.R.*, 1995. Genetic structural provinces and salt tectonics of the
608 Cenozoic offshore U.S. Gulf of Mexico: A preliminary analysis. In: M.P.A. Jackson, D.G.
609 Roberts, and S. Snelson (eds.), *Salt tectonics: A global perspective*. AAPG Memoir, 65, 153–
610 175.

611

612 Porrenga, D.H., 1967. Glauconite and chamosite as depth indicators in the marine environment.
613 *Marine Geology*, 5, 495–501.

614

615 Price, R.A., 1973. Large scale gravitational flow of supracrustal rocks, southern Canadian
616 Rockies. In: DeJong, K.A., and Scholten, R.A. (eds.), *Gravity and Tectonics*. New York, Wiley,
617 491–502.

618

619 Quittmeyer, R.C., Kafka, A.L., 1984. Constraints on plate motions in southern Pakistan and the
620 northern Arabian Sea from the focal mechanisms of small earthquakes. *Journal of Geophysical*
621 *Research*, Solid Earth, 89, 2444–2458.

622

623 Reynolds, K., Copley, A., Hussain, E., 2015. Evolution and dynamics of a fold-thrust belt: The
624 Sulaiman Range of Pakistan. *Geophysical Journal International*, 201, 683–710.

625 Rowlands, D., 1978. The structure and seismicity of a portion of the southern Sulaiman Range,
626 Pakistan. *Tectonophysics*, 51, 41–56.

627 Sarwar, G., DeJong, K.A., 1979. Arcs, oroclinal, syntaxes: the curvatures of mountain belts in
628 Pakistan. In: *Geodynamics of Pakistan* (Abul Farah and Kees A. DeJong eds.), Geological
629 Survey of Pakistan, Quetta, 341–349.

630 Schori, M., Mosar, J., Schreurs, G., 2015. Multiple detachments during thin-skinned deformation
631 of the Swiss Central Jura: a kinematic model across the Chasseral. *Swiss Journal of Geosciences*,
632 108, 327–343.

633 Schwab, F.L., 1986. Sedimentary ‘signatures’ of foreland basin assemblages: Real or
634 counterfeit? In: *Foreland Basins* (ed. by P.A. Allen and P. Homewood), *Special Publication*,
635 *International Association of Sedimentologists*, 8, 395–410.

636 Shah, S.M.I., 2009. *Stratigraphy of Pakistan*. GSP Memoirs, Volume 22, 400 pp.

637 Simpson, G.D.H., 2006a. How and to what extent does the emergence of orogens above sea level
638 influence their tectonic development? *Terra Nova*, 18, 447–451.

639 Sinclair, H.D., Coakley, B.J., Allen, P.A., Watts, A.B., 1991. Simulation of foreland basin
640 stratigraphy using a diffusion model of mountain belt uplift and erosion: an example from the
641 central Alps, Switzerland. *Tectonics*, 10, 599–620.

642 Sinclair, H.D., 1997. Tectonostratigraphic model for underfilled peripheral foreland basins: An
643 Alpine perspective. *Geological Society of America Bulletin*, 109, 324–346.

644

645 Sinclair, H.D., Gibson, M., Naylor, M., Morris, R.G., 2005. Asymmetric growth of the Pyrenees
646 revealed through measurement and modeling of orogenic fluxes. *American Journal of Science*,
647 305, 369–406.

648 Spratt, D.A., Lawton, D.C., 1996. Variations in detachment levels, ramp angles and wedge
649 geometries along the Alberta thrust front. *Bulletin of Canadian Petroleum Geology*, 44, 313–323.

650

651 Sultan, M., 1997. The Stratigraphy, petrography and provenance of the Upper Cretaceous–
652 Paleocene Formations of the Middle Indus Basin, Pakistan. Ph.D. Thesis, University of South
653 Caroline, Columbia, SC, USA.

654

655 Szeliga, W., Bilham, R., Kakar, D.M., Lodi, S.H., 2012. Interseismic strain accumulation along
656 the western boundary of the Indian subcontinent. *Journal of Geophysical Research*, 117.

657

658 Treloar, P.J., Izatt, C.N., 1993. Tectonics of the Himalayan collision between the Indian plate
659 and the Afghan block: A synthesis. In: P.J. Treloar and M.P. Searle (eds.), *Himalayan tectonics*:
660 Geological Society (London) Special Publication 74, 69–87.

661 Wang, Z., Tang, S., Chen, D., Lins, S., Nie, F., 1996. Basic Geological Studies and Preliminary
662 Evaluation of Uranium Potential of Siwaliks in the Middle Part of Sulaiman Mineral Belt
663 Pakistan. An internal report of PAEC, Dera Ghazi Khan.

664

665

666

667

ACCEPTED MANUSCRIPT

1 **List of Figures Captions**

2 **Figure 1.** A. *Shuttle Radar Topography Mission* Digital Elevation Model (SRTM-DEM, 90 m
3 resolution, 3arc-second) derived from USGS-NASA SRTM data, showing the location of the
4 study area, the Sulaiman Fold-Thrust Belt (SFTB) and Sulaiman Foredeep. B. The location of
5 two-dimensional (2D) seismic lines and wells superimposed on SRTM-DEM. Text in yellow
6 shows the exploratory wells drilled in the area for hydrocarbon exploration. (DEM Data
7 downloaded from Jarvis, A., H.I. Reuter, A. Nelson, E. Guevara, 2008, Hole-filled SRTM for the
8 globe Version 4, available from the CGIAR-CSI SRTM 90m Database (<http://srtm.csi.cgiar.org>)

9 **Figure 2.** Tectono-stratigraphic chart of the eastern SFTB compiled from the results of this
10 work.

11 **Figure 3.** a. Seismic stratigraphy of Choti-01 well, indicating the stratigraphic thickening at the
12 Eocene level. b-c. Litho-biologs from Zindapir-01 and Burzi-01 illustrating the lithologic and
13 biofacies information. The presence of planktonic foraminifera is plotted against specified depth
14 intervals. Glauconite is also observed in the Cretaceous-Paleogene strata. The gamma ray (GR)
15 log indicates the lithologic variation (from clean clastic-carbonate intervals to shaley intervals).

16
17 **Figure 4.** Uninterpreted (a) and interpreted (b) seismic reflection profile O-805-SK-18 runs close
18 to Dhodak-05 well. The Dhodak anticlinal structure is interpreted indicating gentle dips. The
19 anticlinal structures are marked by an increase in amplitude anomalies.

20
21 **Figure 5.** Uninterpreted (a) and interpreted (b) dip seismic profile 845-SK-29 lies at a distance of
22 about 41 km from the Zindapir-01 well. The profile illustrates the presence of folded structural
23 geometry indicative of a compressional regime. The presence of structural high with amplitude

24 anomaly is clearly observed. Structural highs observed are favorable hydrocarbon traps while
25 structural lows are possible kitchens.

26 **Figure 6.** Fold wavelength vs stratigraphic thickness plot for folds in the ZP domain. The folds
27 wavelength is compared with the work derived from Morley et al. (2011) on the deep-water fold
28 and thrust belts (FTBs'), though the study area is not a deep-water FTB and is more similar to
29 the Zagros Fold Belt of Iran. The graph shows the wavelength vs. stratigraphic thickness of
30 deformed strata in the SFTB-ZA compared with worldwide shale-detachment associated FTBs'.

31 **Figure 7.** Uninterpreted (a) and interpreted (b) seismic profile 954-FZP-06. Note the presence of
32 Paleogene stratigraphic expansion at 2.6-3.00 sec TWT. The continuous, parallel reflectors
33 suggest deposition in rather a stable shelf environment with no apparent break in slope and less
34 tectonic/structural disturbance in the area. The strata below are the Paleocene succession.

35 **Figure 8.** Uninterpreted, instantaneous phase and interpreted zoomed images from seismic
36 profile 954-FZP-06 indicating the stratigraphic thickness expansion.

37 **Figure 9.** Uninterpreted (a) and interpreted (b) dip seismic section 954-FZP-12, covering the
38 Sulaiman Foredeep tectonic domain. The more or less parallel reflectors suggest deposition in a
39 relatively stable continental shelf environment. (c) The Paleogene progrades are the result of
40 uplift along the flexural bulge caused due to the lithospheric flexure during the Indian-Eurasian
41 plates (Afghan Block) ongoing collision.

42 **Figure 10.** Block diagram showing the tectono-stratigraphic model of the SFTB-ZA and the
43 Sulaiman Foredeep in the study area during the Cretaceous. The model is based on 2D seismic
44 interpretation and well log analysis. The black dots are locations of exploratory wells.

45 **Figure 11.** Block diagram showing the tectono-stratigraphic model of the SFTB-ZA and the
46 Sulaiman Foredeep during the Paleogene. The model is based on electrical logs, drill cuttings
47 from wells and 2D seismic data.

48 **Figure 12.** Block diagram showing the tectono-stratigraphic model of domains SFTB-ZA and
49 the Sulaiman Foredeep during Recent time. This model is based on seismic interpretations
50 coupled with electrical logs.

51 **Figure 13.** Diagrammatic play cross-section across the eastern SFTB showing the tectono-
52 stratigraphic architecture. The section is compiled from the results of this research.

53

54

55

ACCEPTED MANUSCRIPT

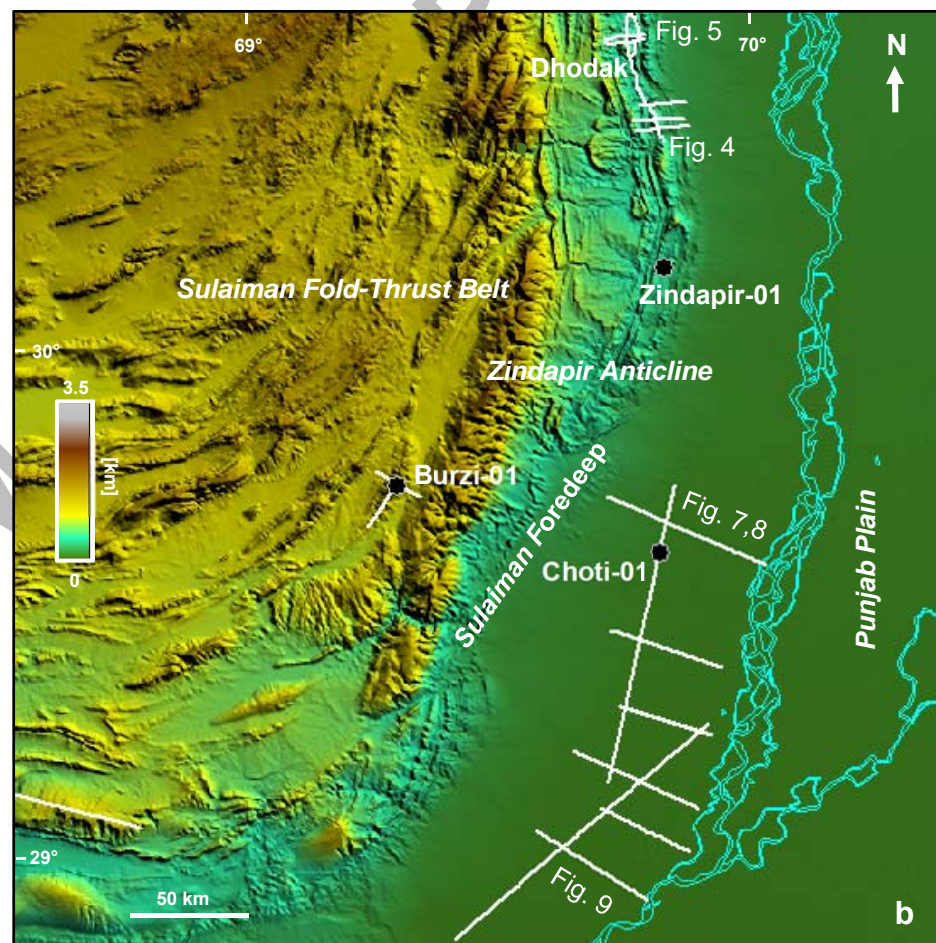
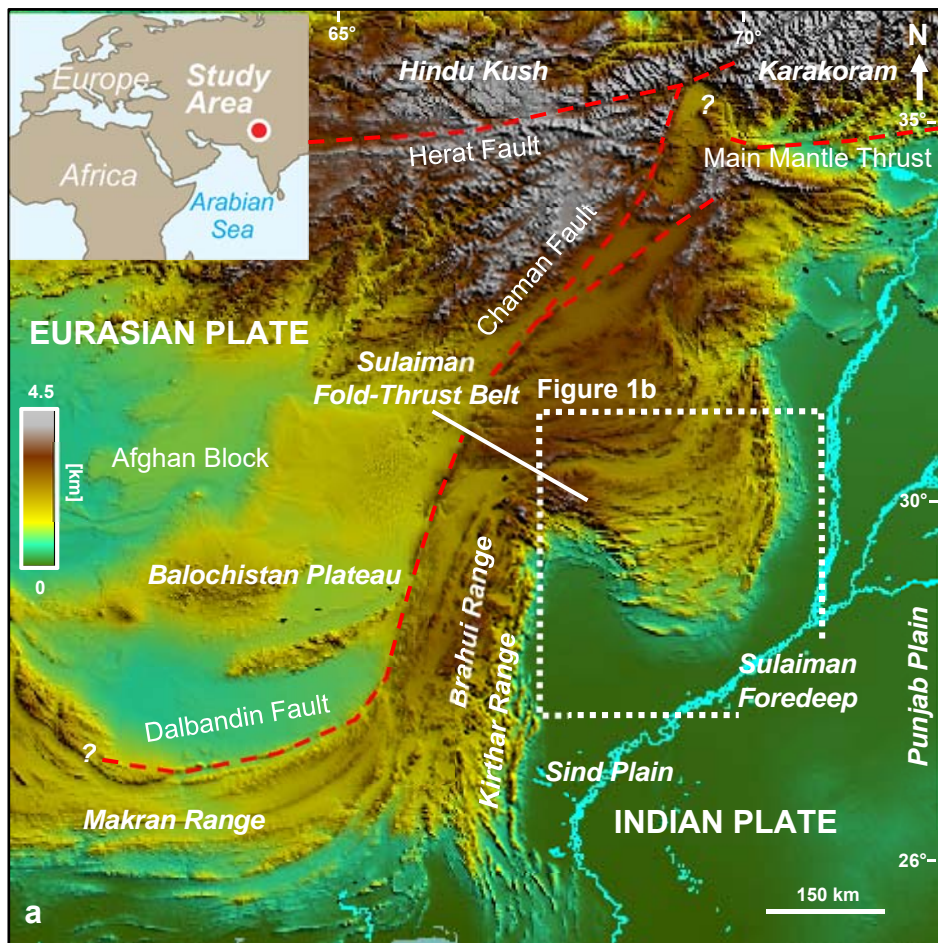


Figure 1.

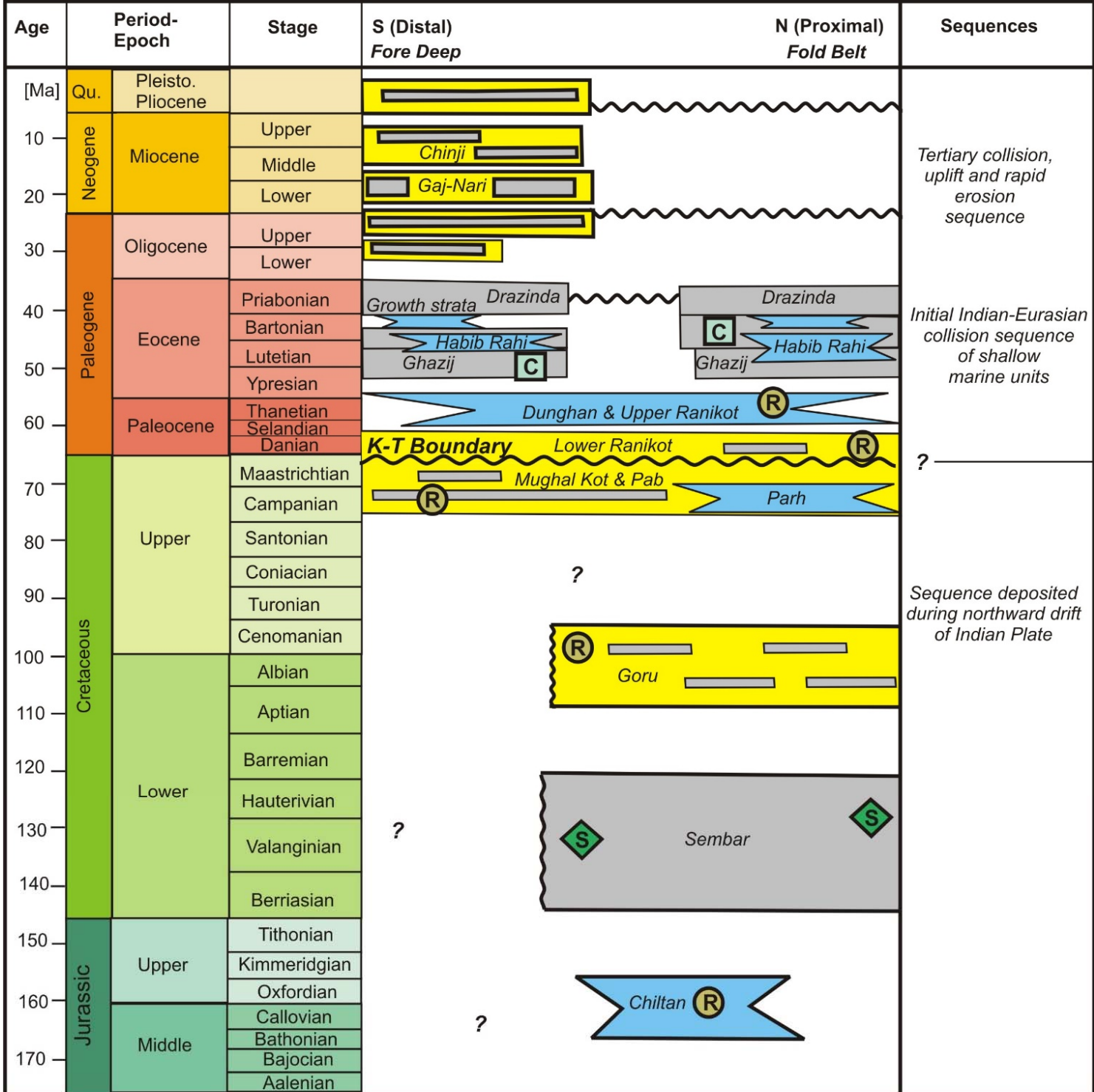
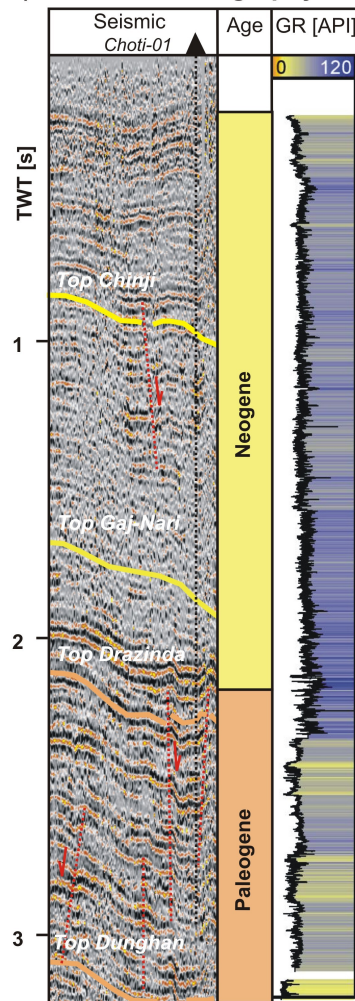
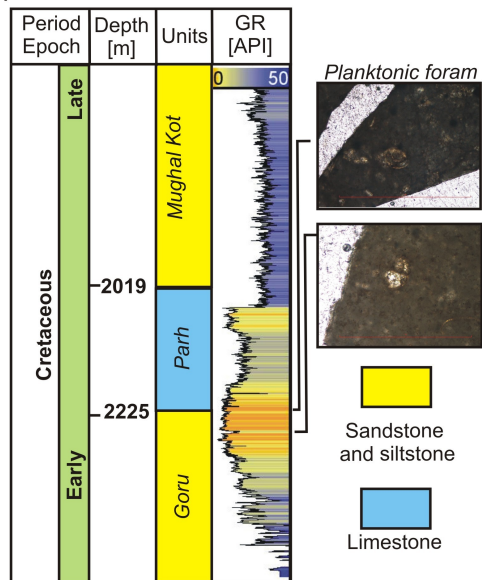


Fig. 2

a) Seismic Stratigraphy



b) Burzi-01



c) Zindapir-01

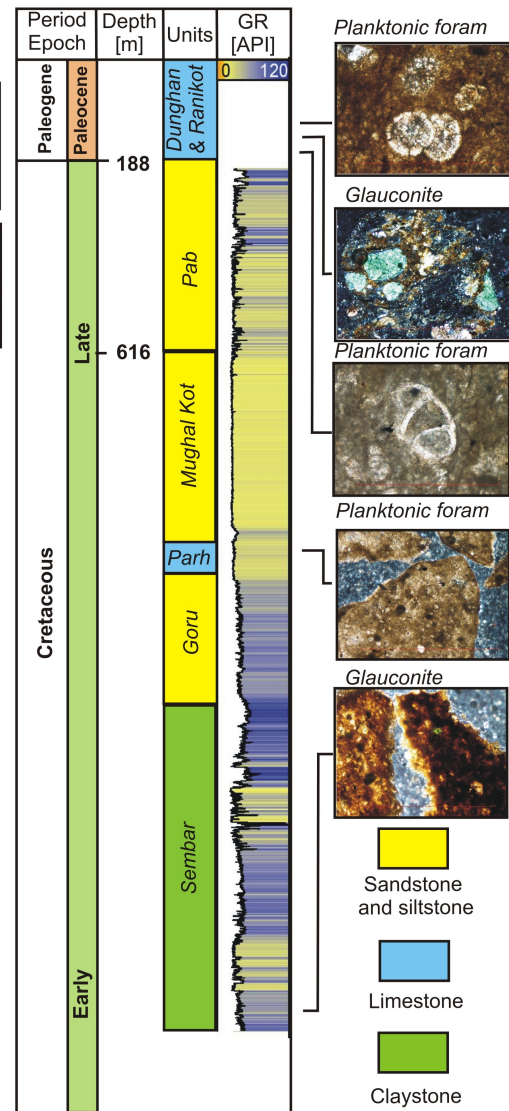


Fig. 3

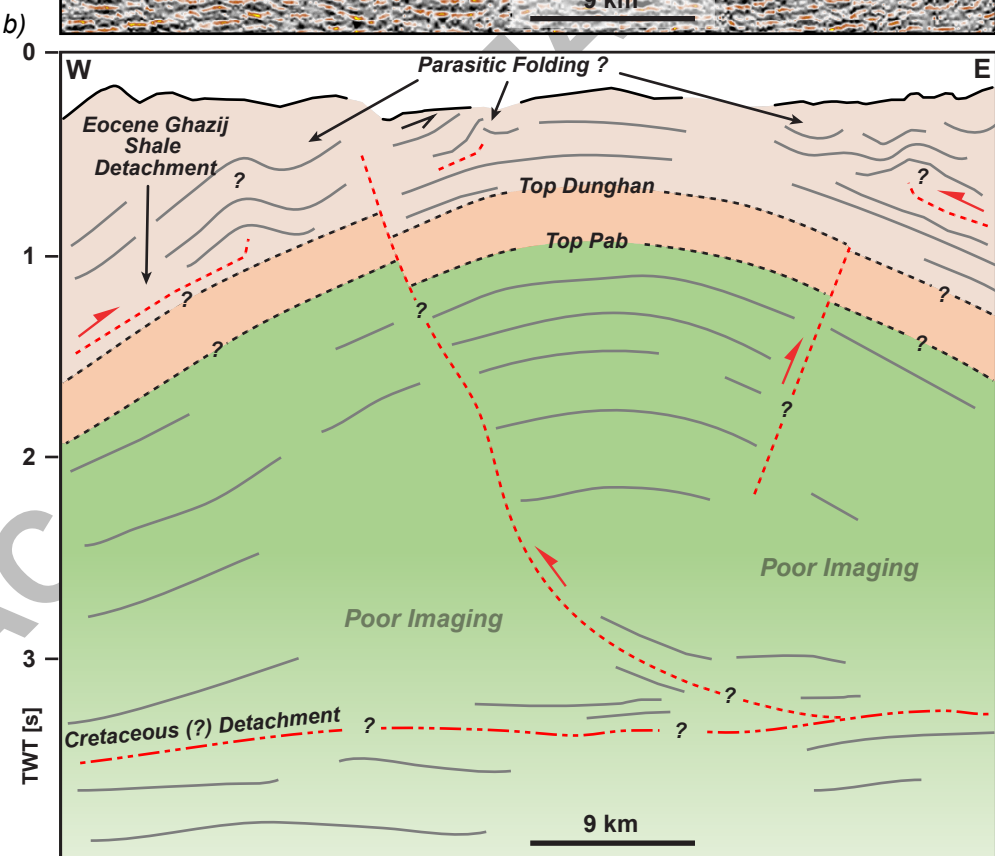
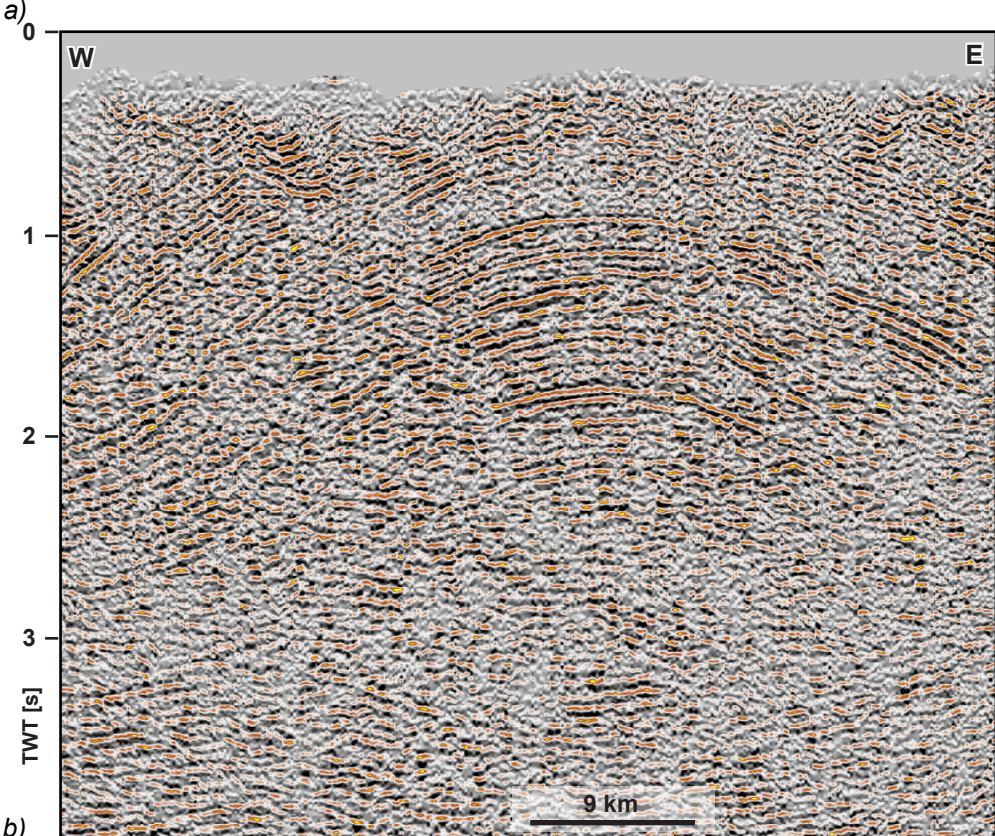



Fig. 4

 Cretaceous and older

 Paleocene

 Eocene

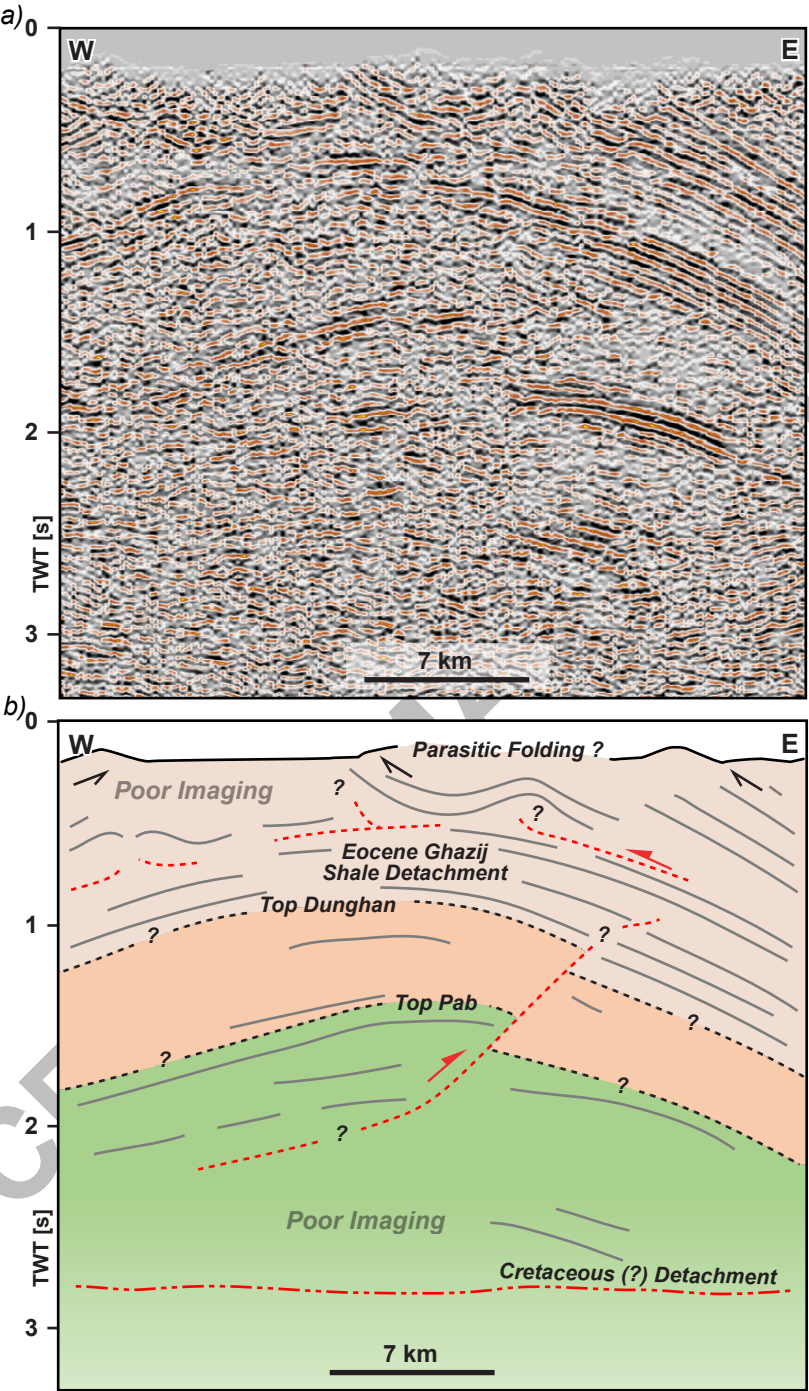


Fig. 5



Cretaceous and older



Paleocene



Eocene

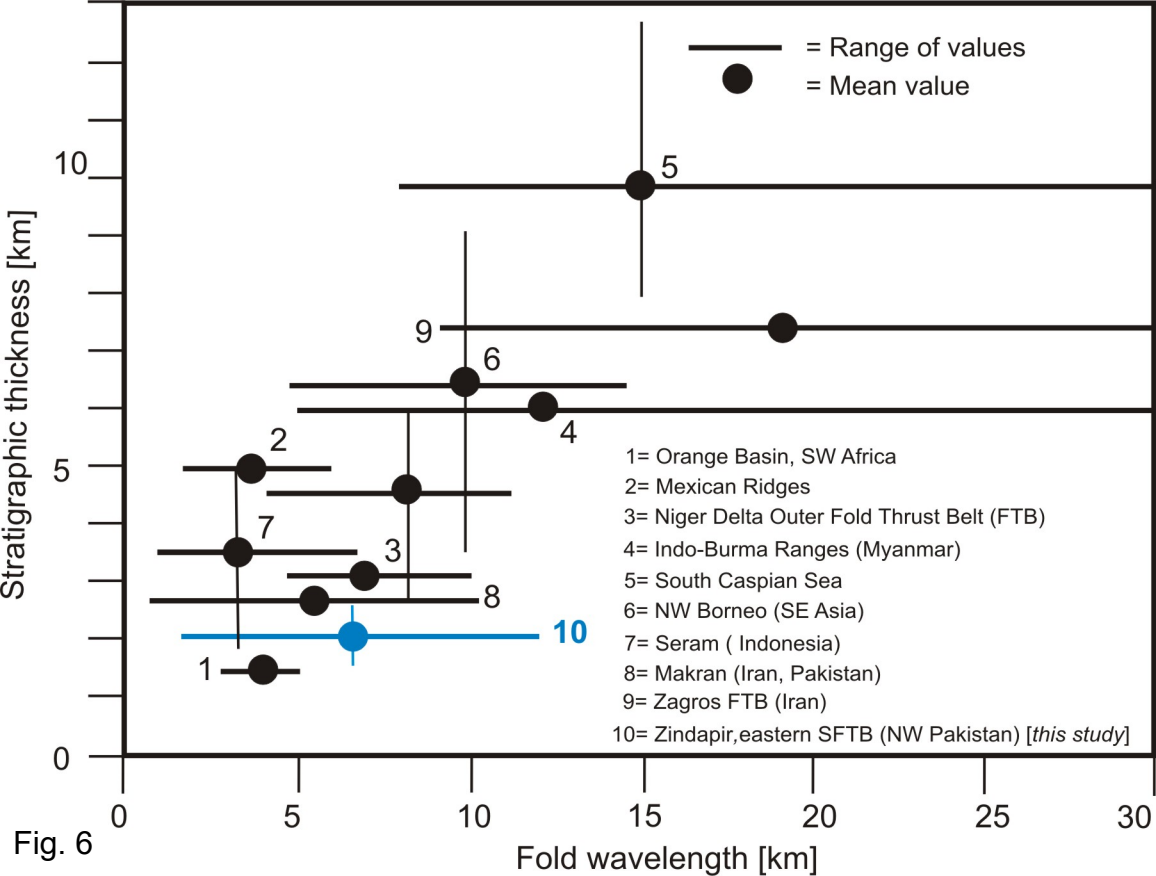


Fig. 6

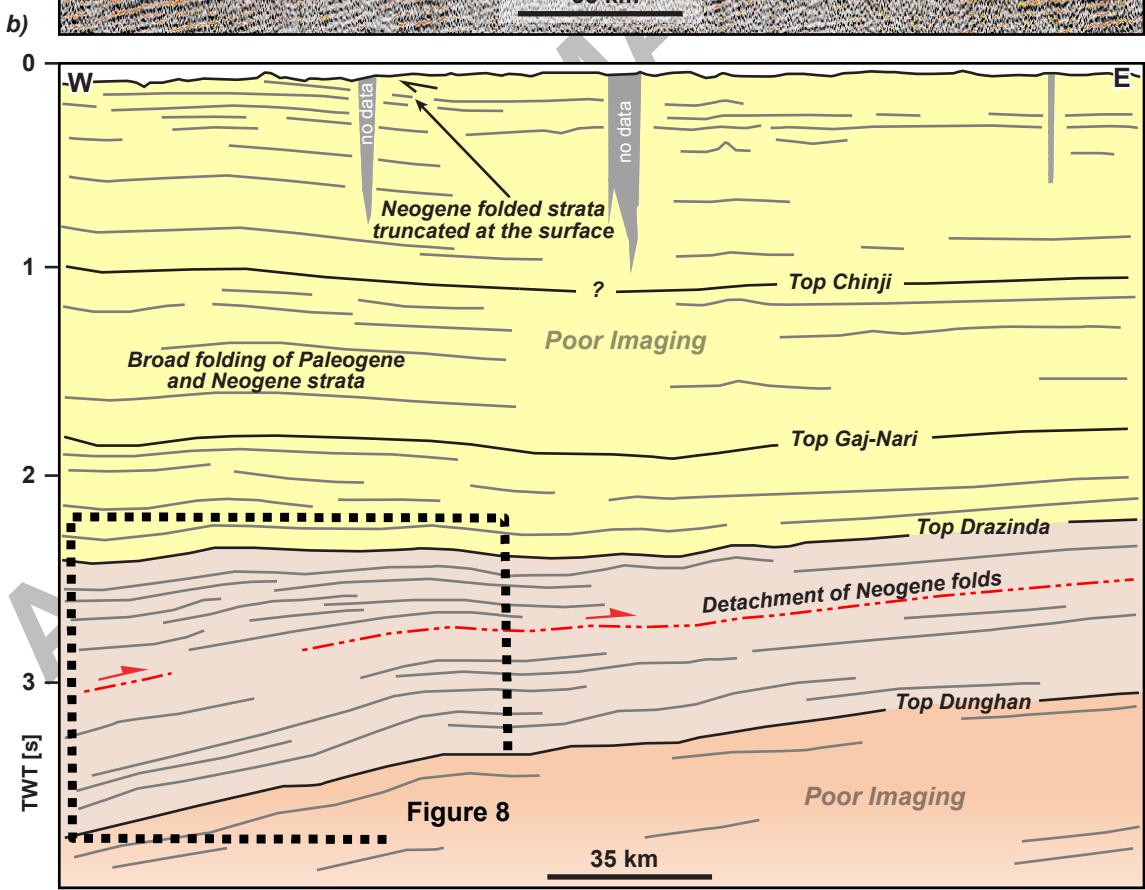
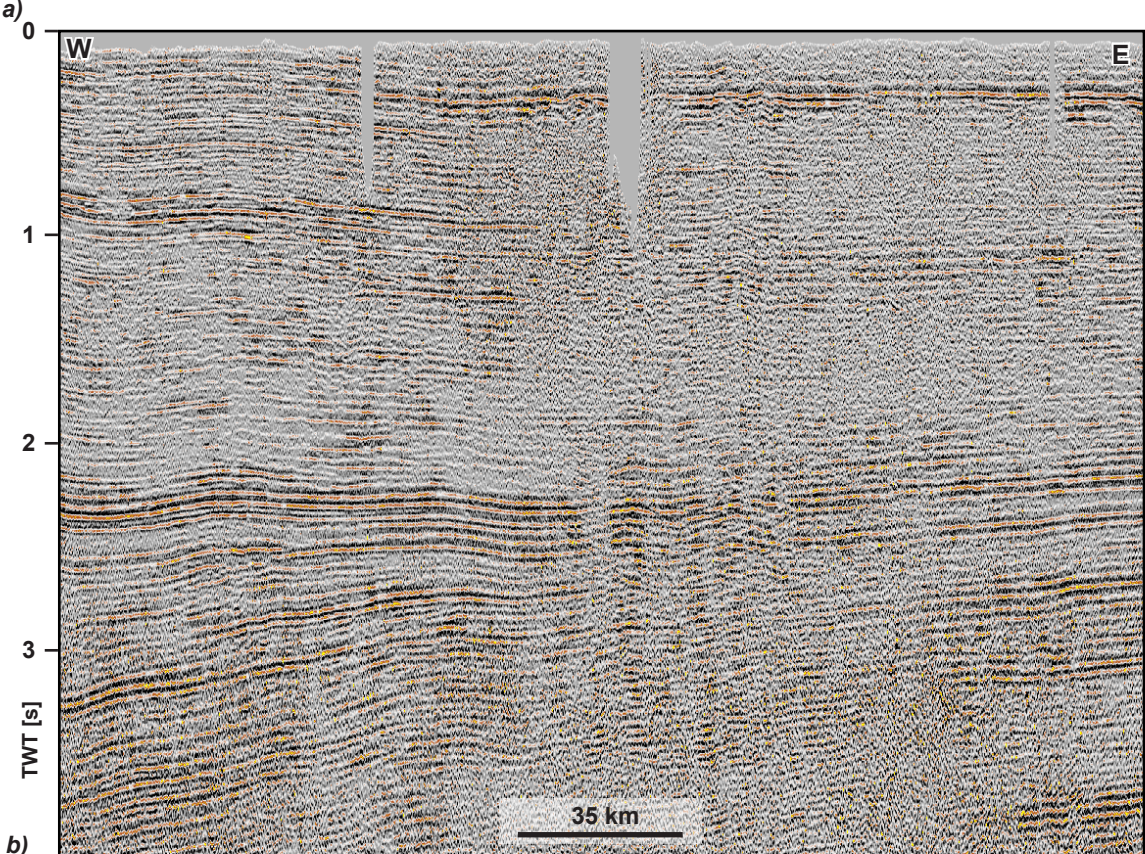


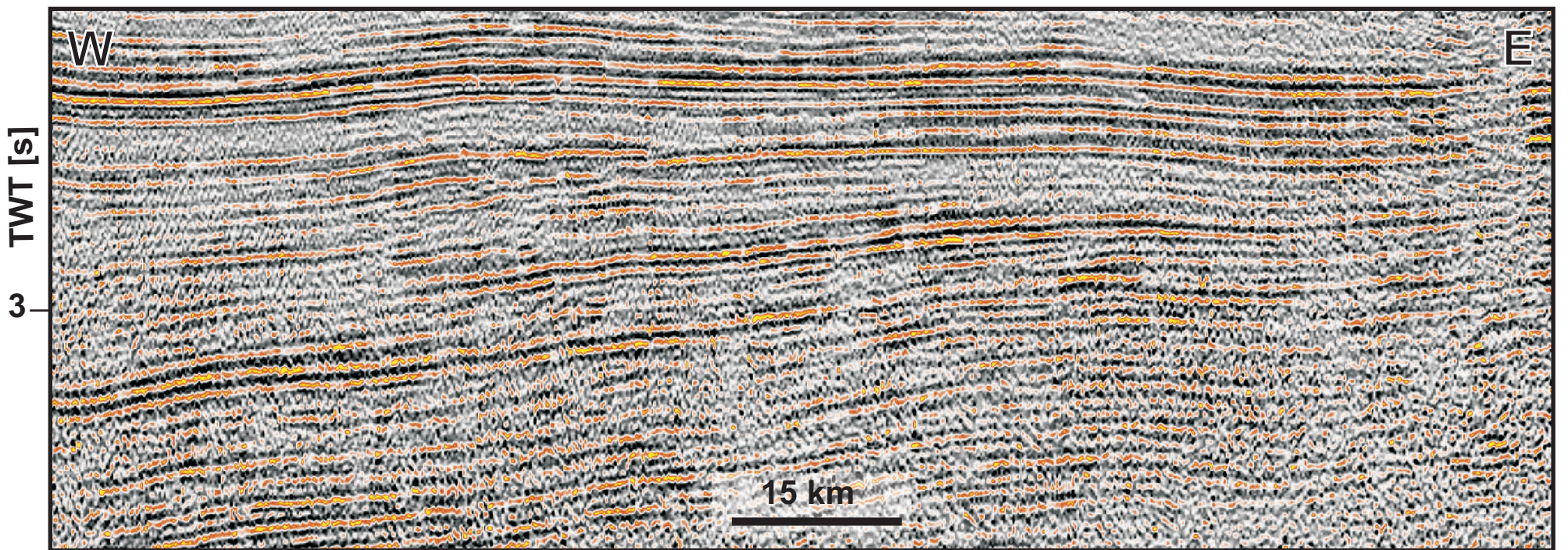
Fig. 7

 Paleocene and older

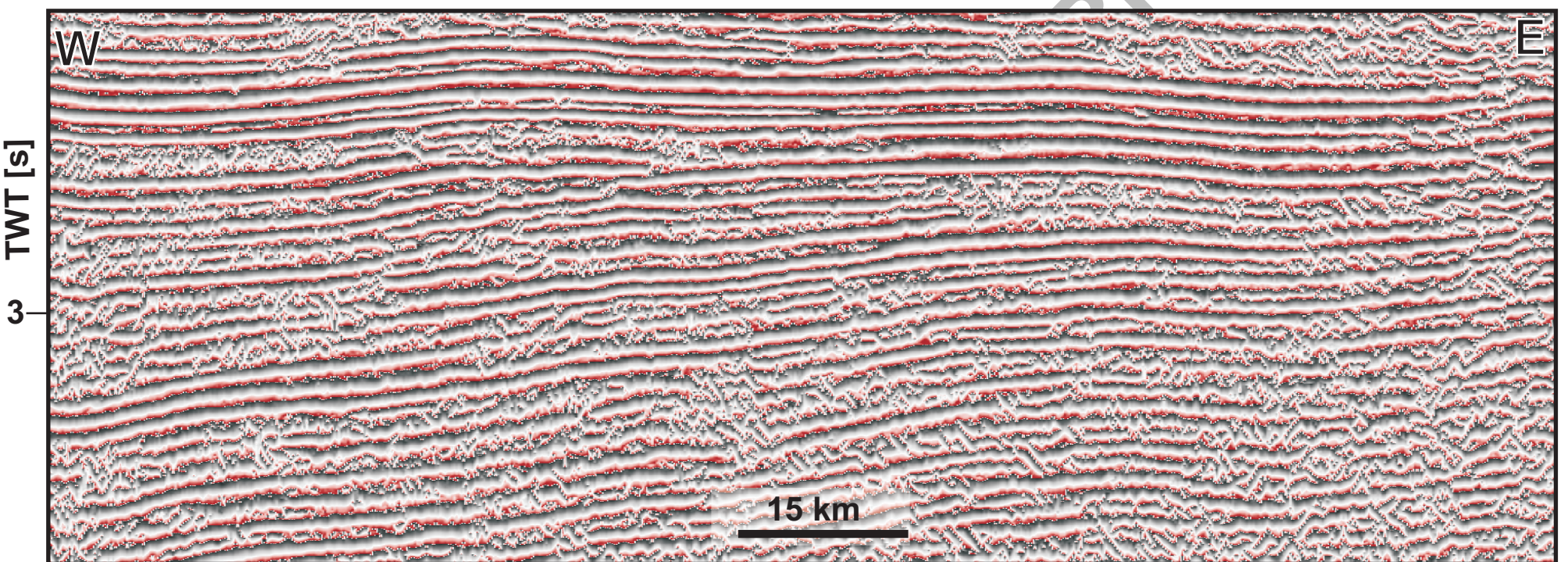
 Eocene

 Neogene

a) Amplitude section



b) Instantaneous phase section



c) Interpretation

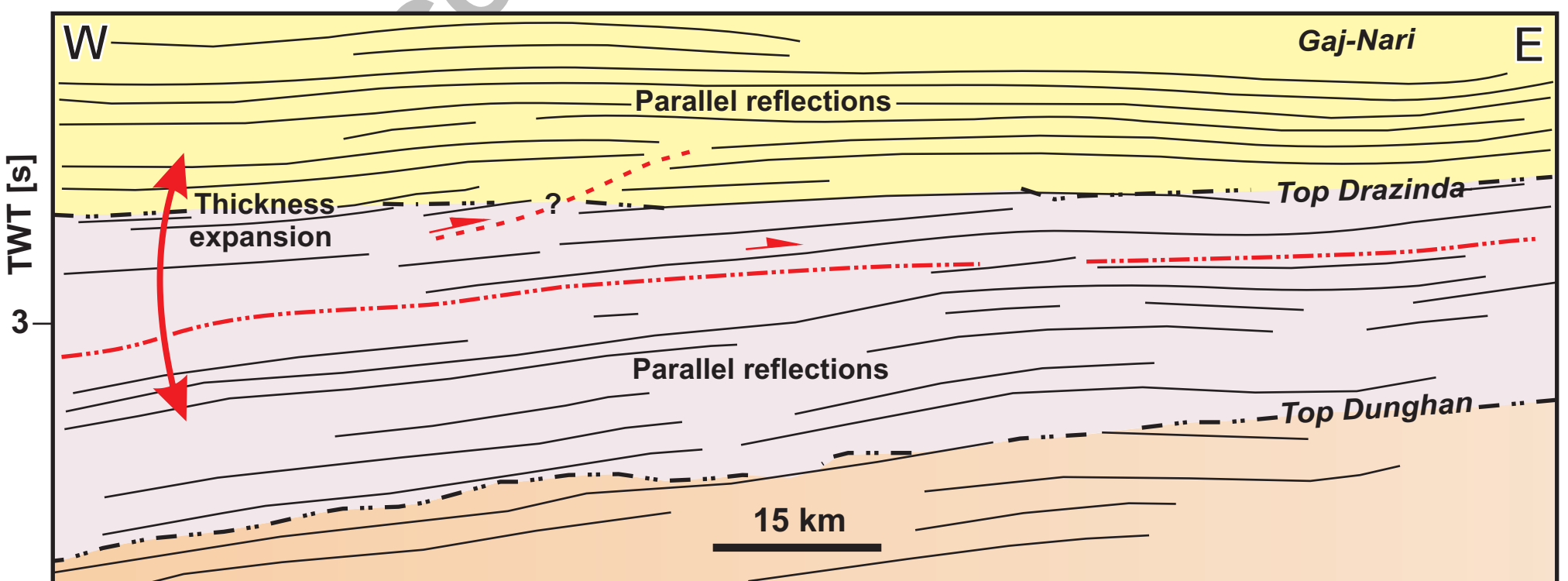
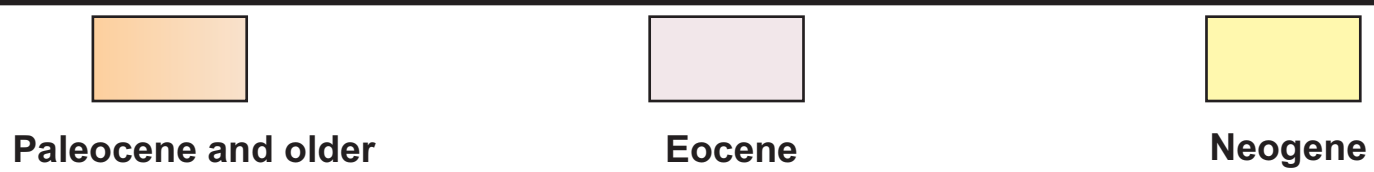


Fig. 8



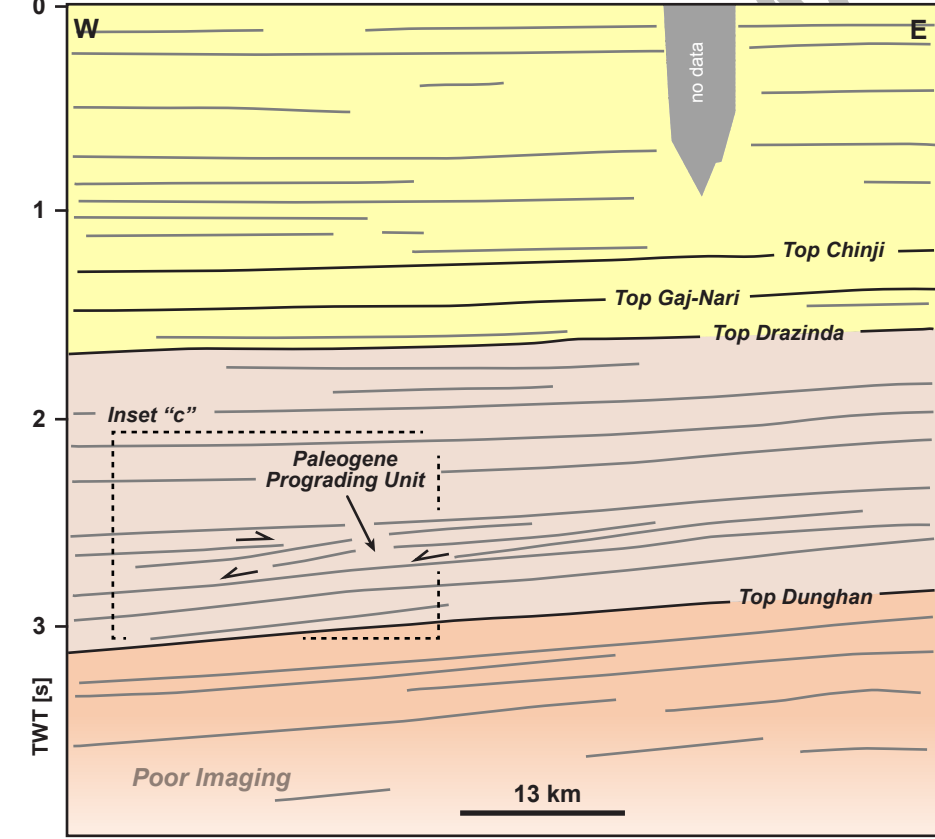
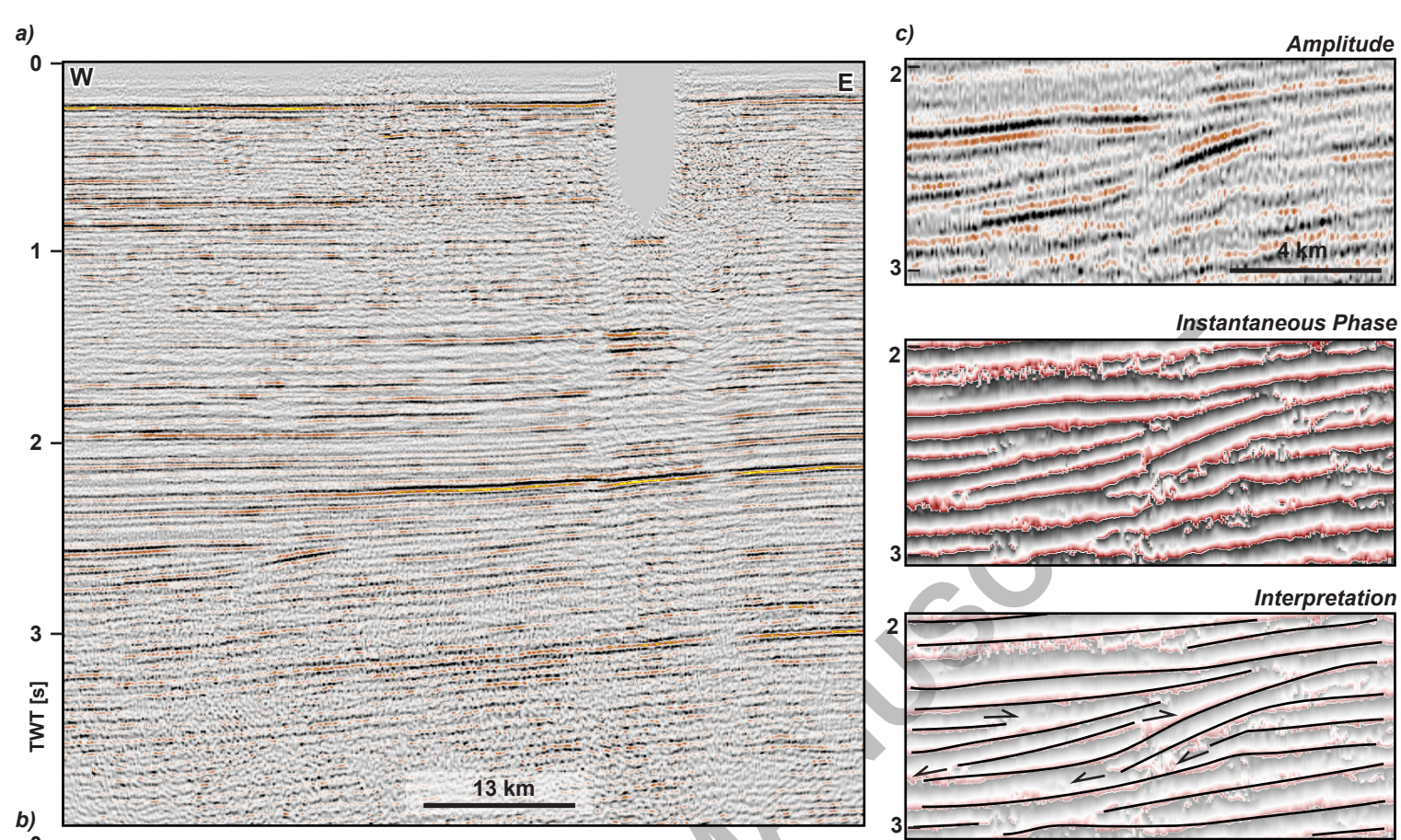


Fig. 9

Late Cretaceous (100-66 Ma)

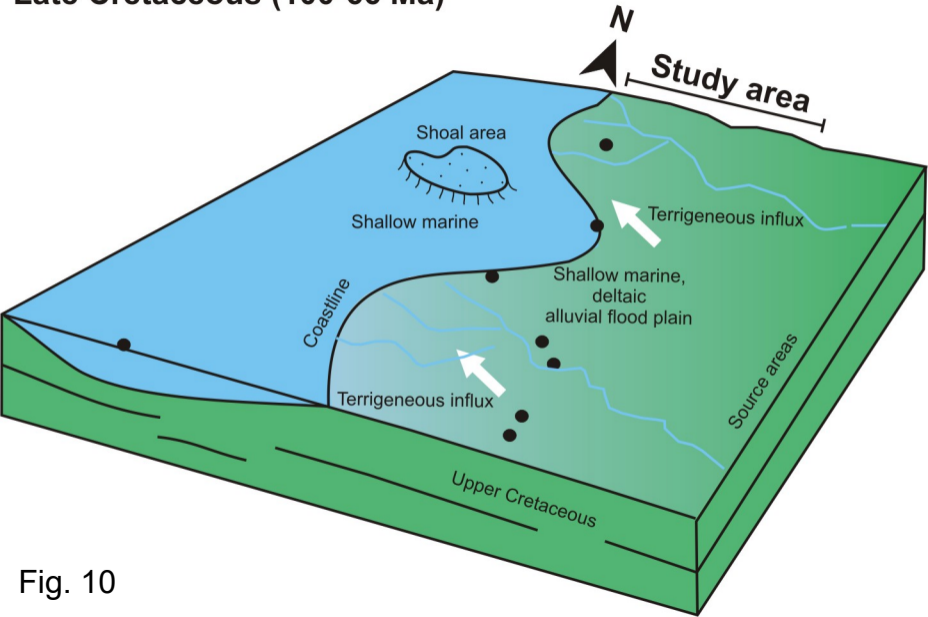


Fig. 10

Paleogene (66-23 Ma)

Onset of compression and associated strike-slip inversion tectonics (NW-SE)

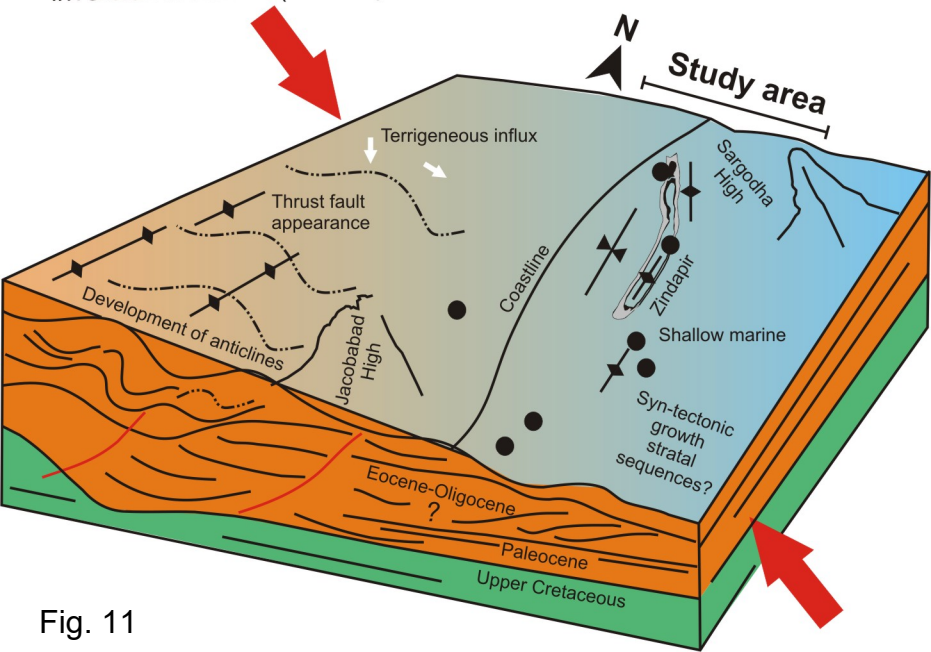


Fig. 11

Present-Day (Recent)

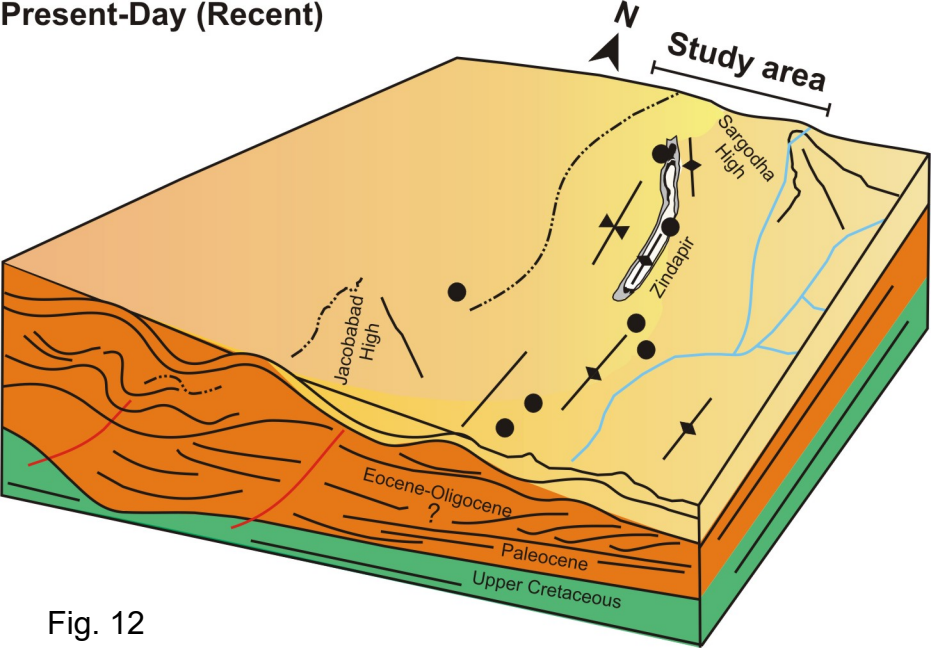


Fig. 12

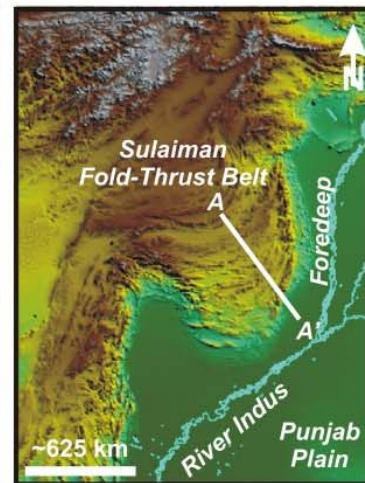
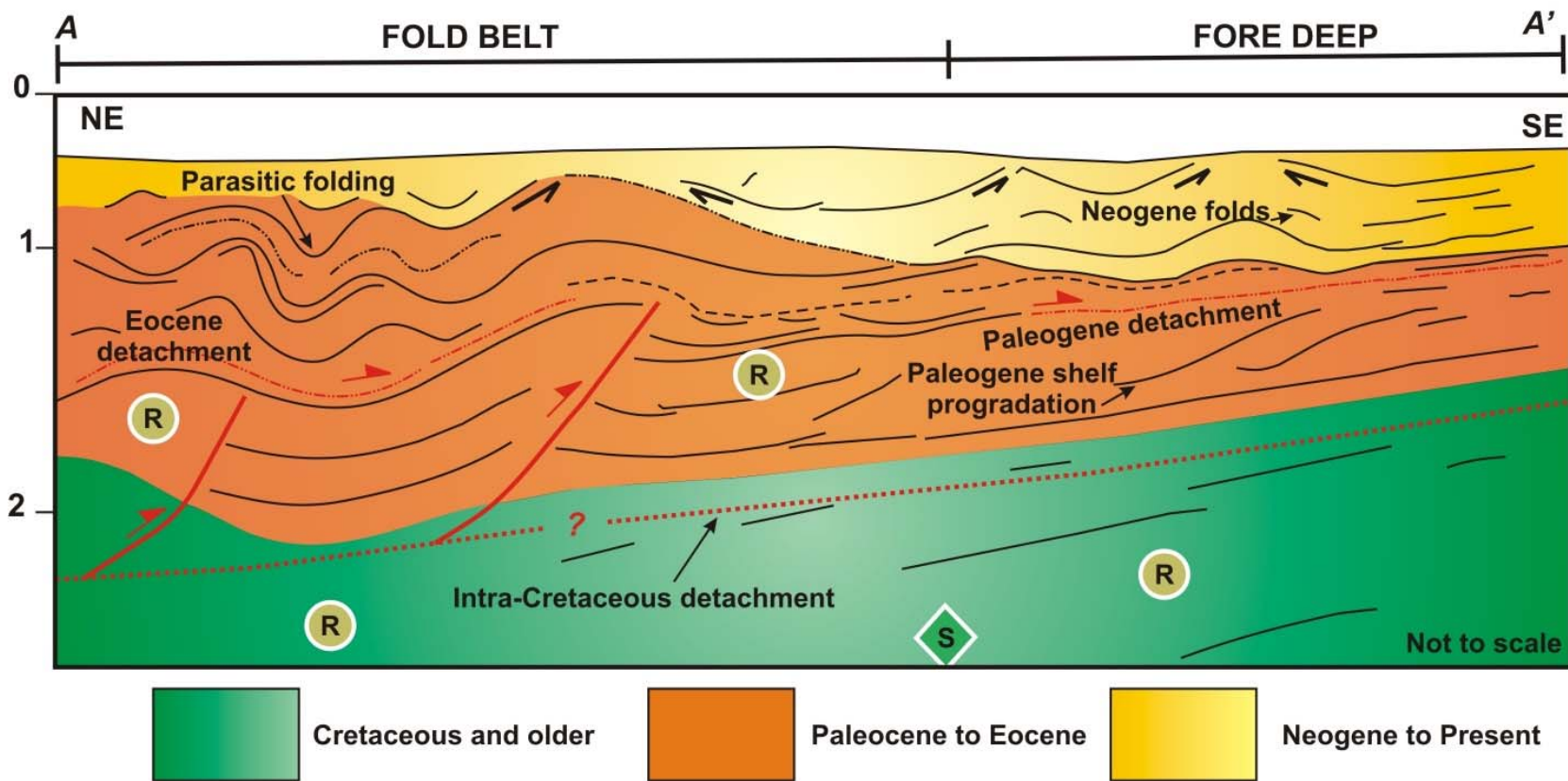


Fig. 13

Table 1. Parameters and characteristics of 2D seismic surveys used in this study (Total: 605.6 LKm (approx.))

Sulaiman Fold Thrust Belt (SFTB)-Western						
Line Number	Length (Lkm) Approx.	Area	Client	Shot point (SP) Range	Data Class	Sample Interval/Rate (sec)
Strike Lines						
O-985-SIK-08	16.2	Siah Koh	NA	200-599.5	Migrated	0.002
Dip Lines						
O-985-SIK-03	13.9	Siah Koh	NA	200-582.5	Section not fully migrated	0.002
O-806-PRK-06EXT	33.5	Pir Koh	OGDCL	64-372	Migrated	0.004
O-816-PRK-06R	9.5	Pir Koh	OGDCL	101-166	Migrated	0.004
Zindapir Anticline (ZA)-Eastern						
Strike Lines						
O-785-SK-04	40	Sufaid Koh	OGDCL	101-326	Migrated	0.004
Dip Lines						
O-795-SK-05R	10	Sufaid Koh	OGDCL	68-180.5	Migrated	0.004
O-845-SK-27	12.9	Sufaid Koh	OGDCL	39-216.5	Migrated	0.004
O-855-SK-31	12.4	Sufaid Koh	OGDCL	38-198	Migrated	0.004
O-805-SK-18	11	Sufaid Koh	OGDCL	101-201	Migrated	0.004
O-805-SK-19	11.6	NA	NA	101-181	Migrated	0.002
O-845-SK-29	14	Sufaid Koh	OGDCL	38-228	Migrated	0.004
O-795-SK-06	16	Sufaid Koh	OGDCL	101-276	Migrated	0.002
Sulaiman Foredeep (SF)						
Strike Lines						
O-954-FZP-05	89.4	Fazalpur	OGDCL	101-1346	Migrated	0.002
Dip Lines						
O-954-FZP-06	45.5	Fazalpur	OGDCL	101-732	Migrated	0.002
O-954-FZP-08	36.6	Fazalpur	OGDCL	1-392	Migrated	0.002
O-954-FZP-09	38.3	Fazalpur	OGDCL	1-458	Migrated	0.002
O-954-FZP-10	42.2	Fazalpur	OGDCL	1-513.5	Migrated	0.002
O-954-FZP-11	26.2	Fazalpur	OGDCL	421-788	Migrated	0.002
O-954-FZP-12	35.2	Fazalpur	OGDCL	102-402	Migrated	0.002
O-954-FZP-13 (Oblique line)	91.2	Fazalpur	OGDCL	101-1371	Migrated	0.002

*OGDCL - Oil and Gas Development Company Limited, Pakistan

*NA - Not available

ACCEPTED MANUSCRIPT

ACCEPTED MANUSCRIPT

